SHEAR BEHAVIOUR OF ORDINARY STRENGTH RC SLENDER BEAMS

(Test on beams with minimal shear and moderate longitudinal

Reinforcement under uniformly distributed load)

By

Asad Abbas Mughal
(NUST201260961MSCEE15212F)

A Thesis submitted in partial fulfillment of

the requirements for the degree of

Master of Science

In

Structural Engineering

NUST Institute of Civil Engineering

National University of Sciences and Technology

Islamabad, Pakistan

(2016)

This is to certify that

thesis entitled

SHEAR BEHAVIOUR OF ORDINARY STRENGTH RC SLENDER BEAMS

(Test on beams with minimal shear and moderate longitudinal

Reinforcement under uniformly distributed load.)

Submitted by

Asad Abbas Mughal

Has been accepted towards the partial fulfillment

Of

The requirements

For

Master of Science in Structural Engineering

_____

Brigadier (Retired) Dr. Khaliq-ur-Rashid Kayani
NUST Institute of Civil Engineering, NUST Islamabad

National University of Sciences and Technology Islamabad

SHEAR BEHAVIOUR OF ORDINARY STRENGTH RC SLENDER BEAMS

(Test on beams with minimal shear and moderate longitudinal

Reinforcement under uniformly distributed load.)

By

Asad Abbas Mughal
(NUST201260961MSCEE15212F)

A Thesis submitted in partial fulfillment of

The requirements for the degree of

Master of Science

In

Structural Engineering

NUST Institute of Civil Engineering

National University of Sciences and Technology

Islamabad, Pakistan

(2016)

To my parents
And well wishers

Table of Contents

LIST OF FIGURES

ACKNOWLEDGEMENT

ABSTRACT

This experimental study was devised to ascertain the effects of longitudinal reinforcement on shear strength of RC slender beams under uniformly distributed load instead of concentrated two point loading which has so far been used to understand and formulate the shear design concept.

Eight RC beams were divided into four groups of two beams each based on ACI minimum criteria, P.D. Zararis hypothesis, modified form of Zararis equation and beams without shear reinforcement for reference and comparison. These specimens were tested under uniformly distributed load with a constant moderate longitudinal reinforcement. Ultimate shear strengths obtained in this experimental program are compared to the analytical shear strengths calculated according to ACI code provisions, Zararis Equation and the Modified Zararis Equation. Test results show that ACI equation for calculating shear strength of RC beams is conservative. Zararis' and Modified Zararis' equations are appropriate for calculating shear capacity of beams. On an additional note a/d ratio was also ascertained for distributed loading which comes to about L/4 for this set of tests.

LIST OF ABBREVIATIONS/NOTATIONS

F'_c Compressive concrete strength

f_y Yield strength of longitudinal reinforcement

f_{yv} Yield strength of shear reinforcement

M Moment

M_n Nominal moment strength according to ACI Code

V Shear force

V_d Dowel force due to longitudinal reinforcement

V_{cr} Critical shear force in beam without stirrups

V_{ccr} Critical shear force in concrete

V_{dcr} Critical shear force in longitudinal steel

V_d Increase in dowel force due to stirrups

l_d Development length

l_t Splitting length

α Factor for development length

s Stirrups spacing

ρ Longitudinal reinforcement ratio

b Beam width

d Effective depth of beam

h Overall height of beam

V_c Shear strength provided by concrete

V_s Shear strength provided by concrete

a   Shear span

V_n Nominal shear strength

A_s Area of longitudinal steel

w/c   Water cement ratio

mm   Millimeter

in   Inch

psi   Pounds per square inch

ksi   Kilo pounds per square inch

γ   Factor for predicting shear force provided by concrete

μ   Factor for calculating modulus of rupture

INTRODUCTION

1.1. General

Bending Moment 'M' and Shear force 'V' are mainly the two agents responsible for the stability of beam. "In the design of reinforced concrete member, flexure is addressed first, leading to the size of the section and arrangement of reinforcement to provide the necessary moment resistance. Shear comes at later phase. Failure due to flexural is gradual while beam abruptly fails due to excessive shear forces.

Shear Design means identifying the location of Shear reinforcement and its quantity required to prevent the abrupt failure. Shear reinforcement is provided in the form of stirrups. These stirrups create a connection flexural tension and flexural compression sides of a member to ensure that the two sides act as a unit mass. Shear failures involve breakdown of this linkage and the opening of diagonal crack in members without shear reinforcement.

In the last several decades, particular emphasis has been put on the necessity of a better understanding of the behavior of reinforced concrete beams failing in shear. Code requirements for the design of members to resist shear, based on minimum values of shearing stresses obtained in tests, formerly were considered to be conservative. However, their safety has recently been questioned, especially after the occurrence of unexpected shear failures in structures which had been designed in accordance with code requirements.

1.2. Shear Design Development

"With this number of tests, one would expect the understanding of the problem to be quite complete. However, this is not the case, there is still much to be learned before the problems may be considered solved" stated by Talbot, one of the

pioneers in the research for shear in reinforced concrete members. He conduct testing of 188 beams under shear loading.

After the Talbot statement, extensive programs of tests have been carried out on beams both with and without web reinforcement. In practically all of these investigations, the beams were subjected to a type of loading that would create regions of constant shear; that is, one or two concentrated loads. Under this type of loading the specimens fail at the section of maximum shear and moment.

In 1902, Morsch[1] predicted that shear stress across a cross section of a reinforced concrete beam with flexural cracks has a constant value from bottom to neutral axis and then varies until it reaches the top. Simple equilibrium relationships can be used to calculate these stresses, provided that the flexural stresses at different longitudinal sections of a beam were known. Morsch and Ritter[2] introduced the Truss Model between 1899 and 1902 which was later followed for many years, neglecting any concrete contribution to shear resistance.

The Universities of Stuttgart (Germany), Illinois (USA), and Toronto (Canada) were primarily involved in this filed. Basing on a great number of experiments, ACI 318 Code was considered accurate till 1955, when the unsafe nature of its shear design provisions existing at that time was illustrated by dramatic collapse of two warehouses used by the US Air Force (Figure 1.2). The beams in these warehouses failed under dead load only, when subjected to a shear stress of 0.5 MPa, whereas ACI code allowed a working shear stress of 0.62 MPa. This would correspond to a failure shear stress of about 1.10 MPa. The investigation of this failure led to recommendations for changes in North American design practice, in particular, a minimum web reinforcement which should always be provided. This triggered extensive research to understand the mechanisms through which cracked reinforced concrete beams transmit shear. Shear force in a region indicates that the moment is changing along the length of the member. According to McGregor [3] the shear force $V=d/dx(T*jd)$ changes either by the tension in the reinforcement changing i.e $d(T)/dx$, which is called beam action, or by the internal lever arm changing along the length i.e. $d(jd)/dx$, which is called arch action.

Kani from the University of Toronto, (1964) [4] carried out a very large experimental study on shear behaviour in which he systematically varied the values of shear span to depth ratio (a/d), longitudinal reinforcement (ρl), and compressive strength (f"c). He reported the relationships between the shear capacity, reinforcement ratio and a/d ratio known as "Kani"s Valley of Shear Failures". Kani, after having carried out a large number of experiments on rectangular beams, classified them into four categories namely; very short, short, slender and very slender beams. He stated that diagonal failure is influenced by a large number of factors like strength and ratio of steel, shape of section, strength of concrete, shear arm ratio, type and detailing of web reinforcement, prestress conditions and direction of loading.

A number of researchers have shown that a/d or M/V*d is an important variable in defining the shear strength of a beam. This effect is explained in a conceptual fashion by equations in Joint ASCE-ACI task committee 426 report and is discussed in ACI-ASCE Committee 326 proceedings. Several researchers have proposed different expressions to predict shear capacity of concrete (Vc) as a function of shear span to depth ratio (a/d) and longitudinal reinforcement ratio (ρl). ACI 318-11 Code specifies equation (11-5) which involves shear strength of concrete (Vc) as a functions of a/d ratio and longitudinal reinforcement ratio (ρl).

Prodromos Zararis (2003)[5] conducted a detailed and systematic study of the shear behavior of RC slender beams and presented a theory based on the mechanism of critical crack which leads to the failure of beam. Equations have been developed basing on the hypothetical theory and comparison of the theory with that of ACI and Eurocode provisions has also been worked out. It has been claimed that concept is more reliable and accurate in predicting the shear capacity of reinforced concrete slender beams. However, experimental validation is required to validate the theory. Zararis also developed the equation for the minimum shear reinforcement by establishing a relationship between shear reinforcement (ρv), shear span to depth ratio and longitudinal reinforcement ratio (ρl).

1.3. Scope

In-spite of much more research on shear behavior of beam. There is a limited research on the beam under uniformly load (fig.1.1) that depicts the actual behavior of beam. Under uniformly loaded beam shear force 'V' varies linearly, while bending
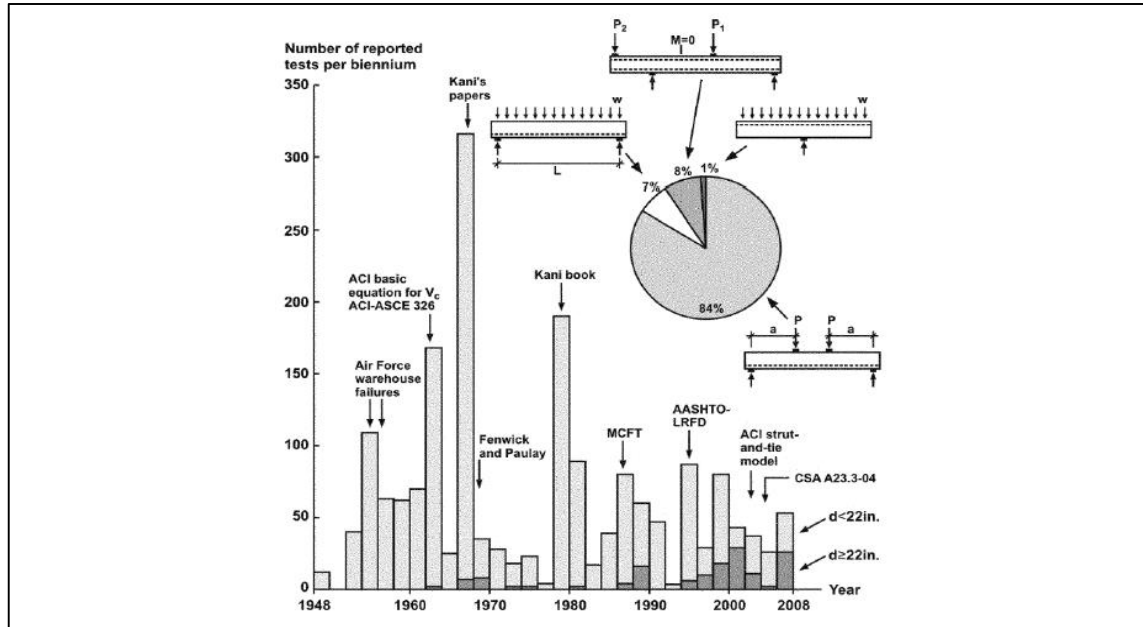
Figure 1.1: Shear Research Trends. Shows the number of reported shear tests per biennium sorted by depth and loading type. From (Collin et al., 2008)

Moment 'M' shows parabolic variation. In this type of loading, the location of section of failure become an additional unknown. The general purpose of this investigation was to explore the behavior and strength in shear of simply supported beams under uniform load.

1.4. Objective

The objectives of the research are:-

➢ To ascertain the accuracy of prevalent expressions for predicting the ultimate shear capacity of reinforced concrete beams under uniformly loaded beams.

➤ To establish minimum shear reinforcement requirement in RC beams incorporating all the factors which effect their shear behavior under uniformly loaded beam.

➤ To develop a relationship between uniformly loaded beams and beams under concentrated loads.

1.5. Methodology

The literature review focusing on available research on shear behavior of RC beams has been carried out. The experimental study based on the review has been devised. Eight full scale beams having moderate longitudinal reinforcement were cast and tested at shear span to depth ratio of 2.5. These samples are described as under:-

➤ Beams without shear reinforcement - 2

➤ Beams with ACI minimum shear reinforcement - 2

➤ Beams with min. amount of shear reinforcement as specified by P.D. Zararis - 2

➤ Beams with minimum amount of shear reinforcement estimated after incorporating changes in Zararis equation – 2

LITERATURE REVIEW

2.1 Shear Strength of Concrete

In a 1935 Engineering News Record review article for structural design engineers, Professor Hardy Cross quoted with approval of the paradoxical statement of the Cambridge astrophysicist Sir Arthur Eddington that "No experiment is worthy of credence unless supported by an adequate theory. (Collins, Bentz, Sherwood and Xie, 2007) [6]

In concrete member when the moment is not constant over its length, shear forces are required to be considered. Almost all flexural members are subjected to shear stresses which may result in diagonal cracks. These diagonal cracks can cause premature failure of the member, which is expected to be a brittle and unstable mechanism. To guard against such phenomenon, appropriate amounts of properly detailed transverse and longitudinal reinforcement should be provided. For determining flexural strength of concrete beams, theory based on Hooke's Law is used which implies that stress is proportional to strain and plane sections remain plane before and after bending. For finding the shear strength of concrete beams, we have following two cases:-

Beams with Shear Reinforcement:

When beams are equipped with shear reinforcement or stirrups, their shear resistance can be ascertained using the truss analogy developed by Ritter and Morsch. The upper bound solution is used to minimize the strengthening effect of the stirrups (Braestrup, 2009) [7].

Beams not having Shear Reinforcement:

In the absence of shear reinforcement, only shear transfer mechanism provides the requisite shear resistance. This primarily is the point where codes of practise lack a theory and use totally empirical procedures. (Collins, Bentz, Sherwood and Xie, 2007) [6]

2.2 Shear Transfer Mechanism

In reinforced concrete beams, shear is transferred by two load transfer mechanisms: beam action and arch action. The contribution of beam action and arch action depends on shear span to depth ratio (a/d ratio). Normally, beam action is the governing load transfer mechanism in slender beams (a/d ratio greater than 2.5) whereas arch action is dominant mechanism in deep beams (a/d ratio less than 2.5). The two shear transfer mechanisms can be expressed mathematically by considering a free body diagram of the portion of a reinforced concrete beam between two cracks as shown in Figure 2.1. Shear force (V) is related to the tensile force in the bar (T) as under:

$$V = \frac{d}{dx}(TJd)$$

$$\Rightarrow V = \frac{d(T)}{dx} + \frac{d(Jd)}{dx}$$
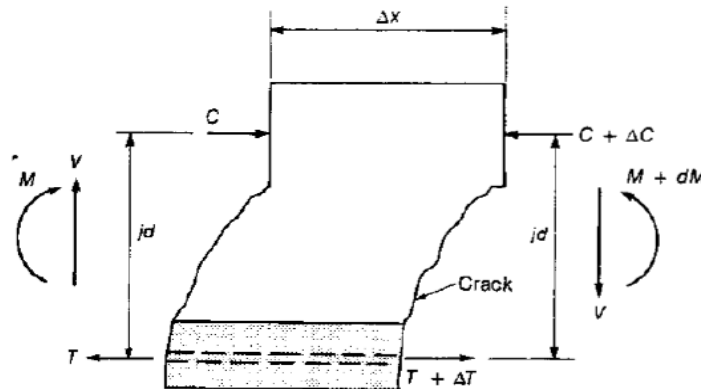
Figure 2-1 : Free body diagram of beam between two cracks (MacGregor) [3]

If the lever arm (*jd*) remains constant as assumed in elastic beam theory, the shear force is transferred in beam action (V$_b$) as follows:

$$\frac{d(Jd)}{dx} = 0 \quad and \quad V = V_b = \frac{d(T)}{dx}$$

Where *V = d(T) / dx* is the shear flow across any horizontal plane between the reinforcement and the compression zone. For beam action to exist shear flow must be

present. On the other hand if the shear flow, $d(T) / dx$ equals zero, then the shear force is transferred to arch action (V_a) as follows:

$$V = V_a = \frac{d(Jd)}{dx}$$

This happens when the reinforcing steel is unbonded and the shear flow cannot be transmitted, or when an inclined crack extend from the load point to the support preventing the transfer of shear flow. In such cases, shear is transferred by arch action instead of beam action (MacGregor) [3].

According to experimental and analytical research, it has been revealed that the primary mechanisms of shear resistance include force provided by concrete in compression zone, aggregate interlock and the dowel action across the longitudinal steel bars. Any shear force, surplus to above three mechanisms, is resisted by steel stirrups which are generally vertically placed and suitably anchored in compression zone to avoid slipping. In a cracked reinforced concrete beam with shear reinforcement, the shear is carried by the vertical component of shear force in compression zone concrete (V_{cy}), Vertical component of aggregate interlock force at the cracked surface (V_{ay}), the dowel action of longitudinal reinforcement (V_d) and the force in the vertical stirrups (V_s). Internal distribution of the forces is shown in Figure 2.2.
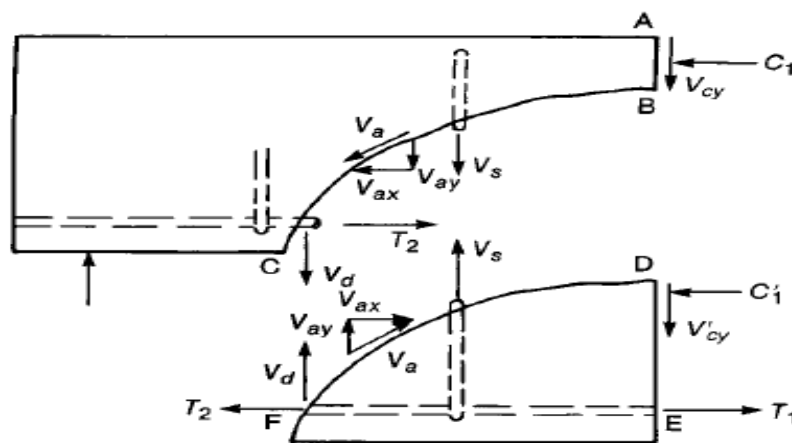
Figure 2-2 : Internal forces in a cracked beam with stirrups (MacGregor)

Distribution of internal shear forces in a beam with web reinforcement, at various stages of loading or applied shear, can be graphically represented as in Figure 2.3
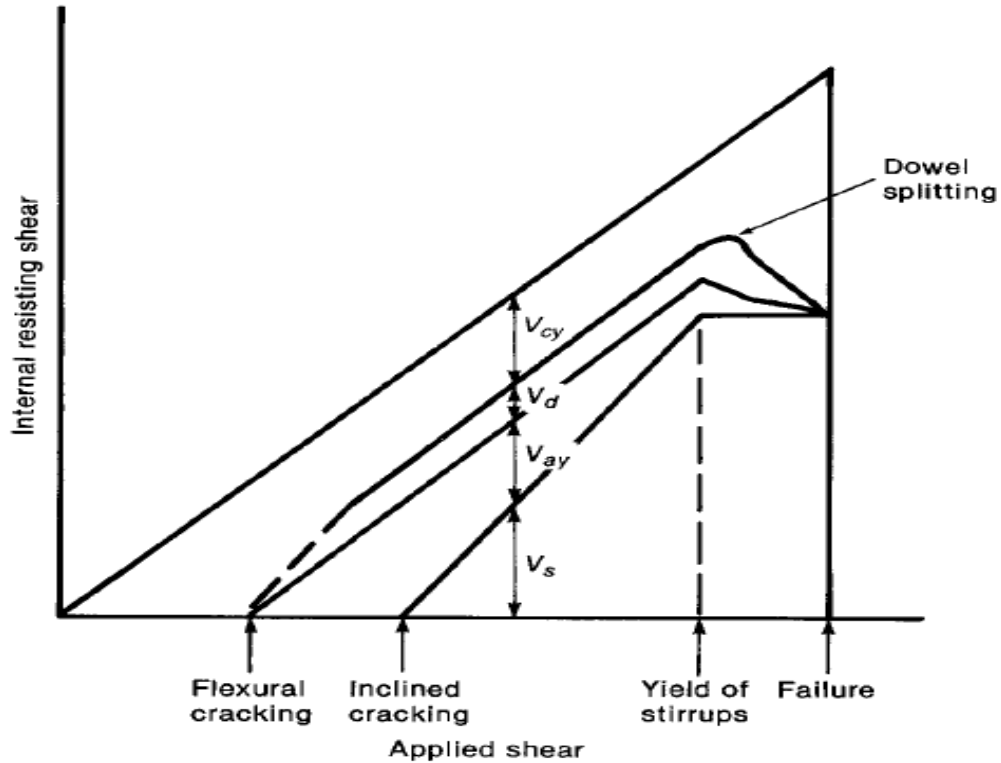
Figure 2-3 : Graphical representation of internal shears in beams

2.3 Shear Theories

2.3.1 Truss Model

Mechanical mathematical models can be used to express the behavior of beams failing in shear. Most suited model for beams with shear reinforcement is the truss model. The Swiss engineer Ritter[2] and the German engineer Morsch[1], in their independent works, proposed the truss analogy for the design of reinforced concrete beams for shear (1899 to 1902). It provided an excellent conceptual model to depict the forces existing in a cracked concrete beam.

Compressive and tensile forces, C and T respectively, are developed in beams with inclined cracks, in its top and bottom portions. Other forces acting in these beams are tension in the vertical stirrups and inclined compressive forces in the concrete

9

"diagonals" between the inclined cracks as shown in (Figure 2.1-Appendix I). This highly indeterminate system of forces is replaced by an analogous truss.

To derive the analogous truss, several simplifications and assumptions are required (Figure 2.2-Appendix I). The truss has been formed by combining all the stirrups cut by section A-A into one vertical member b-c and all the diagonal concrete members cut by the section B-B into one diagonal member b-d. This diagonal member is stressed in compression to resist the shear on section B-B. The compression chord along the top of the truss is actually a force in the concrete but is shown as a truss member. The compressive members in the truss are shown with broken lines and the tensile members with solid lines (Mc Greggor) [3].

2.3.2 Shear Theory

The shear stresses, *v*, on elements of a beam section can be calculated by traditional theory for homogenous, elastic, uncracked beams as:-

$$v = \frac{VQ}{Ib} \tag{2.1}$$

Where,

      V   = Shear force on a cross section

      Q   = First moment about the neutral axis

      I   = Second moment of area of cross section

      b   = Width of member where stresses are being calculated.

It should be noticed that equal shearing stresses exist on both the horizontal and vertical planes through an element (Figure 2.3-Appendix I). The horizontal shear stresses are of importance in the design of construction joints, web-to-flange joints, or regions adjacent to the holes in beams. For an un-cracked rectangular beam, Equation 2.1 gives the distribution of shear stresses.

However, this equation is not applicable to reinforced concrete beams for the following reasons:

- Reinforced concrete comprises two materials having significantly different strength and stiffness and is thus heterogeneous.

- Concrete is subjected to creep therefore, it is not elastic.

- Cross sections of the beams may be cracked or uncracked. Since the extent of cracking at a specified location along the length of the beam is unpredictable, the actual cross sectional properties on which to base computations of moment of inertia and moment of area etc can not be accurately determined.

- Because of cracking, the effective cross section of reinforced concrete members is variable along their length.

Because of the above-mentioned reasons, correct evaluation of shear stress intensity in a reinforced beam is not possible. The ACI 2011 has therefore adopted a simple procedure for establishing the order of magnitude of the average shear stress on a cross section. The shear stress is computed by dividing the shear force by $b_w\,d$, the effective area of concrete.

$$v = \frac{V}{b_w d} \tag{2.2}$$

Where, v = Shear stress at a section

V = Shear force at section

b_w = Beam width

d = Distance between top surface and centroid of bottom steel

2.3.3 Modified Compression Field Theory (MCFT)

It has been shown by researchers that, the inclination of the concrete compression is not necessarily 45 degrees, and that a more realistic basis for shear design is provided by equations based on variable angle truss. Moreover, tests of reinforced concrete panels subjected to pure shear improved the understanding of the

stress-stain characteristics of diagonally cracked concrete. An analytical model called the modified compression field theory was developed by utilizing the concrete stress-stain relationship. This model has proved to be capable of accurately predicting the response of reinforced concrete subjected to shear. Load transmission in cracked reinforced concrete comprises relatively complex mechanisms involving opening or closing of pre-existing cracks, formation of new cracks, interface shear transfer at rough crack surfaces, and significant variation of stresses in reinforcing bars due to bond, with the highest steel stresses occurring at crack locations. The modified compression field model attempts to capture the essential features of this behavior without considering all of the details. The crack pattern is idealized as a series of parallel cracks all occurring at angle θ to the longitudinal direction. The shear stress that can be transmitted across the crack is a function of the crack width w, aggregate size a, and is given as (Mitchell and Collins) [8].

$$V_{ci} = \frac{2.16\sqrt{f_c^{/}}}{0.3 + \dfrac{24w}{a + 0.63}}$$
(2.3)

2.4 Parameters influencing Shear Strength

2.4.1 Shear Span to Depth Ratio (a/d)

The average shear stress at failure is progressively larger for deeper members (a/d ratio below 2.5) rather than in slender beams. This is because of the fact that, in deep members, shear can be easily transmitted directly to the support by means of compression struts. If a direct compression strut will be formed, the conditions on the supports become important. When a member is loaded on the top face and supported on the bottom face, it is more likely to form such a strut (Adebar 1994) [9]. The strut-and-tie model approach should be used for designing the members in which a direct compression strut is expected to form, rather than a sectional design procedure. Furthermore, the *a/d* ratio is used to describe a shear failure mechanism of simply supported, plain concrete beams, loaded with point loads. That was the result that

Leonhardt and Walter (1966) [10] observed after testing beams cast with normal strength concrete.

2.4.2 Depth of Members or Size Effect

Many tests on the shear behaviour of relatively small beams have been carried out in the last decades. It was revealed that the results of these tests cannot be directly applied to full size beams. Kani (1967) [11] showed that for members without shear reinforcement, there is a very significant size effect on the shear strength of these members. The shear strength of these members tends to decrease with the increase in effective depth. This fact was reaffirmed by Shioya. Figure 2.4 explains the effect of size of the member on shear strength. Primary reason for this size effect is believed to be increased widths of diagonal cracks.
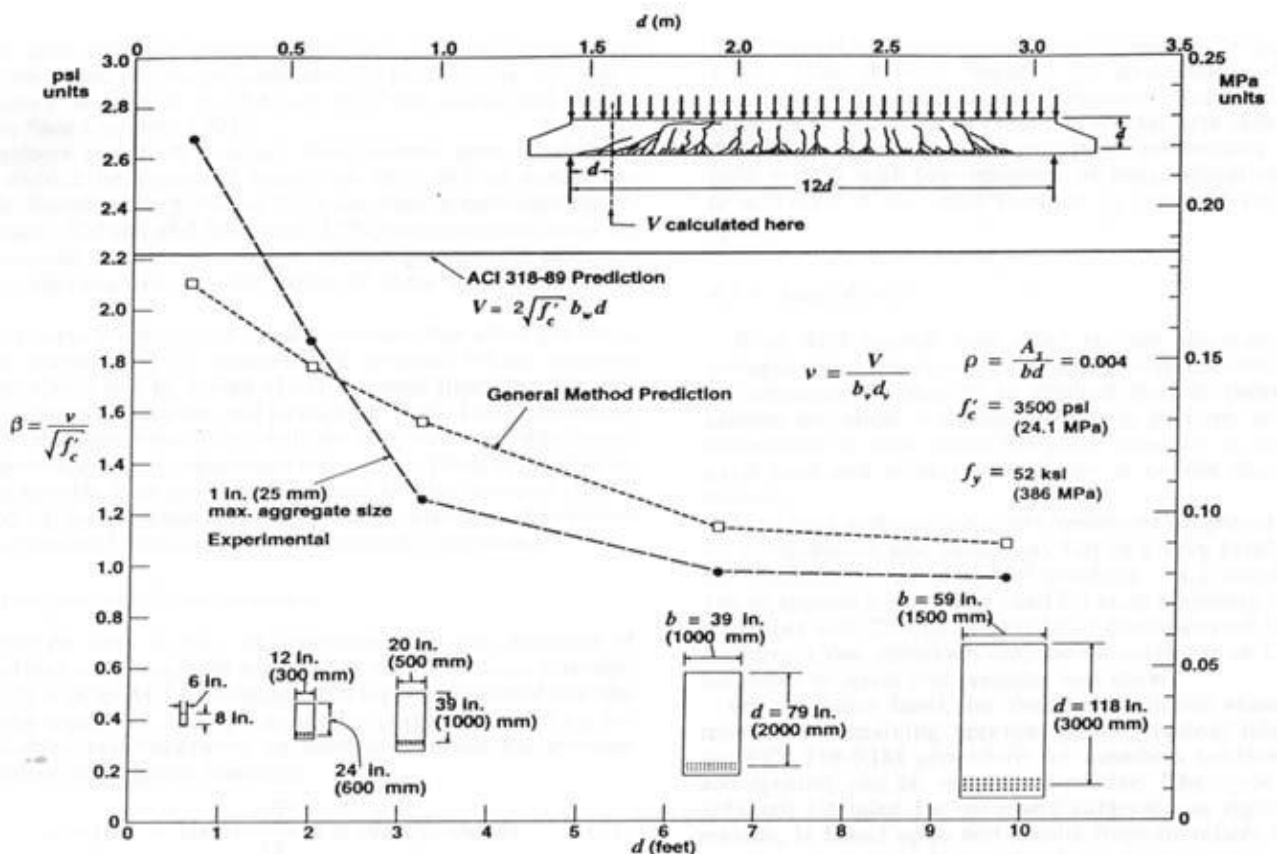
Figure 2-4 : Comparison of large Scale Beam Tests by Shioya et al. with predictions from ACI Code and Modified Compression Field Theory (MCFT).

2.4.3 Axial Force

Shear strength is also dependent on axial force particularly for members without transverse reinforcement. The shear strength of members deceases with an axial tension and increases with an axial compression which may be in the form of applied load or pre-stressing. However, extent of effect of axial force on shear capacity and ductility of the member is still a point of debate in the research community. Very brittle failure is expected in members subjected to axial compression and shear even at the time of initial diagonal cracking. Collins and Gupta (1993) [12] had shown that the ACI Code approach may not be conservative for members subjected to shear and axial compression. Axial load affects the magnitude of shear at the onset of flexural cracking, which was found by Mattock (1969) [13]. The diagonal cracks in members appear to be less than 45° when axial compression is present. Therefore use of the design approach for web reinforcement based on the truss analogy with 45° struts is conservative.

2.4.4 Longitudinal Reinforcement

Kani investigated the influence of longitudinal steel ratio on shear behaviour of members. It is important to note that, although, a higher amount of steel improves the shear response of a member, it definitely makes the failure more brittle and sudden. Kim and Lee (2008) [14] have conducted tests on 26 reinforced concrete beams with minimum shear reinforcement. In their study, reserve strength has been defined as the ratio between the ultimate shear capacity of the beams with the minimum shear reinforcement and that of the beams without shear reinforcement. Likewise, reserve deflection is defined as the ratio between the deflection corresponding to the ultimate load of beams with minimum shear reinforcement and the deflection of beams without shear reinforcement. They had concluded that the amount of minimum shear reinforcement needs to increase / decrease as ρ_l decreases / increases to achieve uniform reserve strength and deflection. It is worth mentioning that, from structural design point of view, a good reinforcement ratio ρ should be balanced after taking into account both shear and flexure mechanisms.

2.4.5 Concrete Compressive Strength

As a result of eleven test series conducted on rectangular reinforced concrete beams by Kani, he concluded that the shear strength does not depend on compressive strength of concrete. However, it should be noticed that Kani tested beams with compressive strength ranging from 18 to 36 MPa. Later studies revealed that the effect of compressive strength is quite noticeable in high strength concretes. Now, it is strongly believed that concrete compressive strength fc' has a significant effect on the ultimate shear strength of concrete members, since shear forces are resisted by concrete and transverse reinforcement. It is not theoretically possible to assess the individual components which describe the concrete contribution to shear. Some researchers (Taylor) [15] have attempted to determine experimentally each of these components for Normal strength concrete (NSC). They have shown that in case of NSC, compressive strength is normally less than the crushing strength of the aggregates. Therefore, the crack skirts across the aggregates. This means that, due to the uneven and jagged surface of the crack, the aggregate interlock component of shear resistance is enhanced. Some researchers and designers are doubting that High strength concrete (HSC) may not be strong in shear because of the aggregate interlock mechanism, which may be absent in HSC. Due to the smaller difference in the strength of aggregates and the concrete matrix, the crack surfaces are smoother compared to NSC (Konig 1993) [16], which means that the aggregate interlock between the fracture surfaces will be reduced. Some tests done by Pendyala and Mendis (2000) [17] showed that the shear strength of concrete beams does not increase significantly in the range of 30 to 70 MPa. In a study by Reineck et al [18], beams made with 100 MPa concrete failed at about the same shear stress as beams made from 35 MPa concrete.

2.4.6 Other Parameters

Besides the parameters described above, other parameters not considered so crucial by the researchers but can affect the shear resistance of a member are as under:-

- Load conditions

- Cross section shape
- Distribution of longitudinal reinforcement

2.5 Failure Modes in Shear

2.5.1 Diagonal Failure

Several structural concrete members like slabs, columns, beams and corbels etc have also been reported to have failed due to shear distress or diagonal failure. Mechanism of transfer of shear in all members is believed to be the same, however, cracking pattern may vary. Diagonal failure is caused due to a combination of shear force and the bending moment (Ziara, 1993) [19].

2.5.1.1 Diagonal Tension Failure

The diagonal crack initiates from the last flexural crack formed. In case of slender beams (a/d between 2.5 and 6), failure occurs within the shear span (a). The crack propagates through the beam and reaches the compression zone and at critical loading, it is likely to fail as a result of splitting of concrete there which is expected to happen suddenly in a brittle manner as shown in Figure 2.5 (Ziara, 1993) [19].

Figure 2-5 : Diagonal tension failure

2.5.1.2 Shear Tension Failure

The difference between diagonal tension failure and this type is that it applies to short beams. In this case too, the shear crack propagates through the beam but is not

likely to cause the failure at its own. Loss of bond between concrete and longitudinal steel can also cause failure due to splitting cracks developing in this region (Figure 2.6). On reaching a critical loading point, beam fails as a result of splitting of the compression concrete (Ziara, 1993) [19].

Figure 2-6 : Shear tension failure

2.5.1.3 Shear Compression Failure

Contrary to shear tension failure, if splitting cracks do not appear and the failure is caused merely due to diagonal shear crack propagating through the beam, it is termed as a shear compression failure (Figure 2.7). This failure mode mainly applies to deep beams. In short beams, due to presence of arch action, the ultimate load causing failure can be much larger.
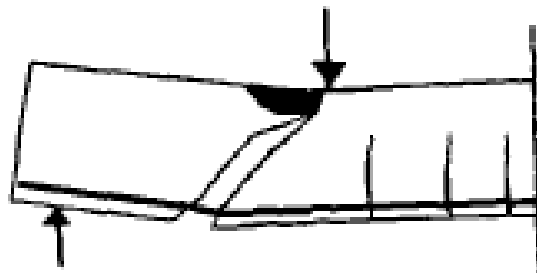
Figure 2-7 : Shear compression failure

2.5.2 Flexural Failure

Moment is basically responsible for initiation and propagation of flexural cracks which occur in slender beams. AT the location where moment in the beam is maximum, appearance of cracks is more likely (Figure 2.8). When the shear stress in the concrete reaches its tensile strength, cracks develop. Flexural cracks are almost vertical and

17

cause failure to the beam either due to excessive yielding of longitudinal reinforcement in case of under reinforced beams, which may cause failure of concrete in tensile zone or due to crushing of concrete in compression zone before the longitudinal reinforcement yields (Ziara, 1993) [19].
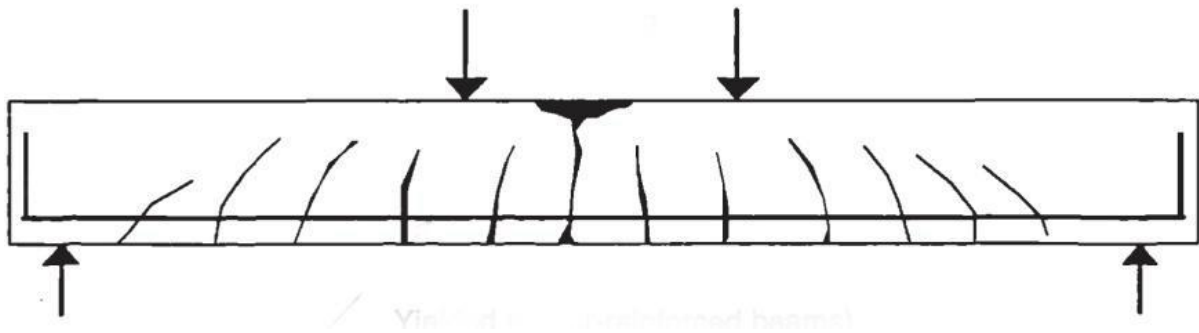
Figure 2-8 : Flexural failure

2.5.3 Anchorage Failure

Anchorage failure may be described as a slip or loss of bond of the longitudinal reinforcement (Figure 2.9). It can be linked to dowel action where the aggregates interlocking resistance around the bar has failed resulting in splitting of the concrete.
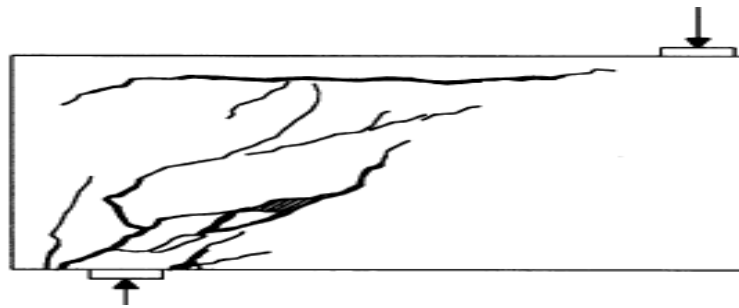
Figure 2-9 : Anchorage failure

2.5.4 Bearing Failure

When bearing stresses exceed the bearing capacity of the concrete, it results in failure of the support. If size of bearing plate is too small, it will result in failure if concrete at the support as in Figure 2.10.
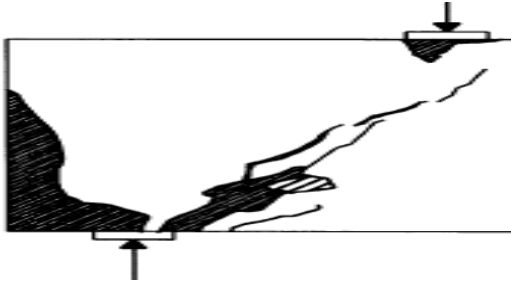
Figure 2-10 : Bearing failure

2.6 Minimum Shear Reinforcement

To avoid abrupt shear failure, ACI 318 – 11 specifies that minimum amount of shear reinforcement must be there in reinforced concrete beams. This minimum amount of transverse steel is intended to restrain the growth of diagonal cracks to avoid abrupt shear failure. Basing on previous experimental data for beams of normal and high strength concrete, ACI equation for minimum shear reinforcement has been developed. This equation is believed to have little consideration for the effects of longitudinal reinforcement and shear span to depth ratio (Lee & Kim 2008)[14].

When minimum amount of shear reinforcement is provided in the beams, it holds the two cracked faces together, thus preventing the loss of shear transfer by aggregate interlock. Where required, the minimum shear reinforcement shall be computed by the equations (ACI Section 11.4.6.3) reproduced below. Eq 2.4 is new in the code and was introduced in ACI 318-05 to account for the influence of compressive strength of concrete.

$$A_{v,\min} = 0.75\sqrt{f'_c}\,\frac{b_w s}{f_{yt}} \tag{2.4}$$

But not less than

$$A_{v,\min} = 50\frac{b_w s}{f_{yt}} \tag{2.5}$$

ACI code restricts the spacing between shear reinforcement to half of effective depth or 24 inches for non prestressed members. This condition ensures interception of potential diagonal crack by at least one vertical stirrup.

2.6.1 Diagonal Crack Width and Minimum Shear Reinforcement

When the principle tensile stress at some location reaches the cracking strength of concrete, a crack is formed in the concrete. This crack is normal to the direction of principal tensile stress. In case of members under pure axial tension or to pure flexure, the principal tensile stresses are parallel to the longitudinal axis of the member and cracks form perpendicular to the member axis. The principle tensile stress directions are inclined to the longitudinal axis of the member if the cross section of a member is subjected to shear stresses. A crack is formed at a location where significant shear stresses exist, and is inclined to the member axis. Such cracks are termed as diagonal cracks.

The inclination, spacing and width of the diagonal cracks cannot be predicted by calculating principle stresses in an uncracked beam, rather, it depends on many factors including flexural and shear reinforcement ratios, size and shape of cross section, shear stresses and mechanical properties of concrete and steel. This implies that the inclined cracking width can be calculated using empirical equations, based on empirical works only (Jensen / Lapko 2009) [20]. Various research studies as mentioned below have been carried out to find the empirical expression for determining crack widths.

- Placas and Regan (1971) [21] concluded that maximum crack width is directly proportional to spacing of stirrups and inversely proportional to A_v, $(f'_c)^{1/3}$ and d.
- Bentz, Vecchio and Collins (2006) [22], reasoned out in MCFT that crack width is equal to the product of crack spacing and principal tensile strain.
- More recently, Muttoni and Ruiz (2008) [23] stated that critical crack width is proportional to the product of longitudinal strain in the control depth (*0.6 d*) times effective depth of element.

2.7 Zararis Theory of Critical Shear Crack

Prodromos D. Zararis[5] has carried out a comprehensive and systematic research on shear behaviour of reinforced concrete slender beams both with and without shear reinforcement under concentrated loads as well as uniformly distributed

loads (UDL) and evolved a theory which describes the diagonal shear failure in slender beams. The theory has also been compared with the known experimental results. This theory explains the shear behaviour of beams and provides empirical equations to determine the ultimate shear capacity and minimum shear reinforcement for reinforced concrete slender beams required to restrain the growth of diagonal cracking and prevent a brittle failure.

2.7.1 Beams without Shear Reinforcement

In slender beams loaded under two or single point loading, failure occurs due to critical diagonal crack. Such crack is composed of two distinct branches as in Figure 2.11. First one is an inclined shear crack having height almost similar to flexural cracks. The second branch initiates from the tip of the first branch and propagates towards the load point crossing the compression zone, with its line meeting the support point (Figure 2.12). Second branch which also involves splitting of compression zone concrete is believed to be responsible for failure. This splitting is not similar to the one occurring in the common split cylinder test.
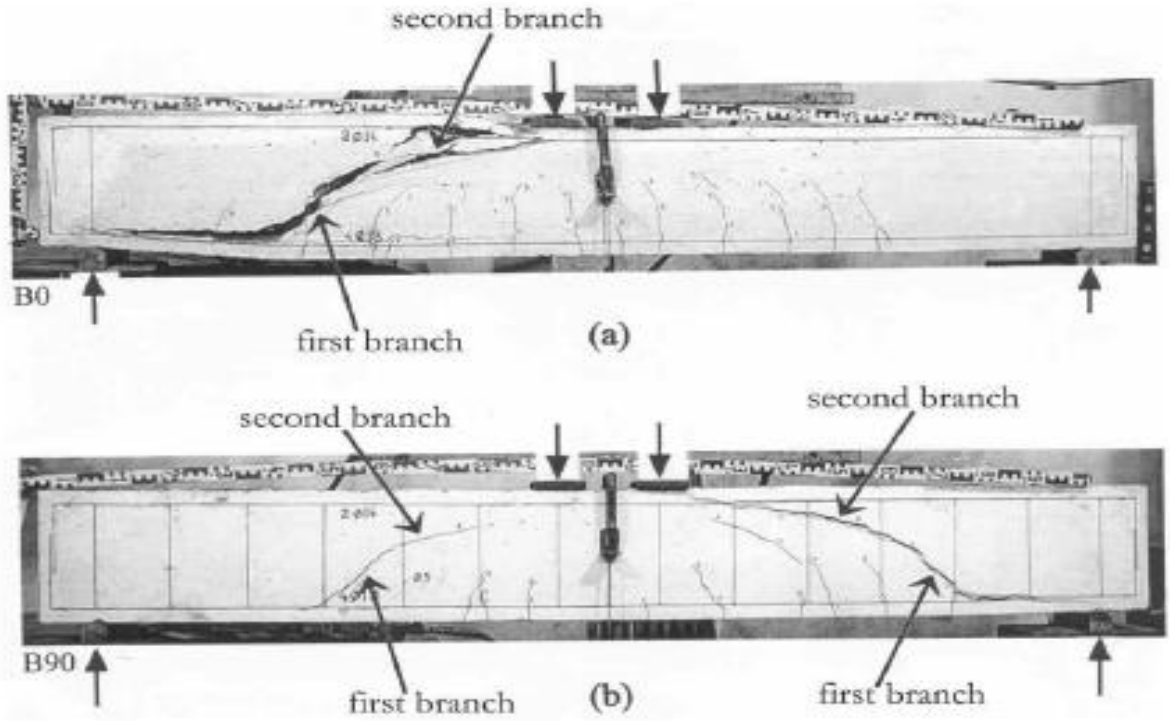
Figure 2-11 : Cracking pattern of slender beams

Nominal shear stress 'v_{cr}' at diagonal tension cracking can be calculated by a simple expression derived in this research as $v_{cr} = V_{cr}/bd = (c/d)f_{ct}$. Moreover, to cater for the size effect on the shear strength, it introduces a correction factor as under:-

$$v_{cr} = \frac{V_{cr}}{bd} = (1.2 - 0.2(\frac{a}{d})d)*(\frac{c}{d})f_{ct} \qquad (2.6)$$

where,

$$1.2\text{-}0.2(a/d)d \geq 0.65 \text{ (d in m)}$$

Taking into account that $a = (a/d)d$, the size effect in beams appears to depend not only on the depth d, as is commonly believed, but also on the ratio *(a/d)*.

22
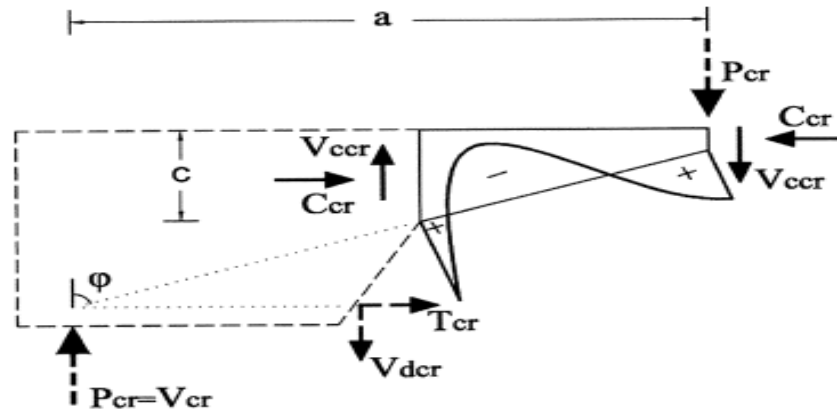
Figure 2-12 : Stress distribution along line of splitting (+: tension, -: compression)

On formation of second branch, dowel force in longitudinal reinforcement 'V_{dcr}' significantly increases. This results in horizontal cracking of concrete cover along main reinforcement. This cracking finally causes loss of 'V_d'. At this point, complete shear force is resisted by compression zone concrete which eventually fails because of shear as shown in Figure 2.11a.

2.7.2 Beams with Transverse Reinforcement

The pattern of cracking of slender beams with stirrups is similar to that of beams without stirrups. The critical crack, in both cases, typically involves two branches, which are formed in the same region of beams. It is reasonable to consider that the causes of formation of the second branch as well as the corresponding cracking load are identical in both cases. Up to the formation of the second branch, the effect of stirrups can be considered negligible. When the formation of the second branch is complete, the concrete shear force V_{ccr} in the compression zone above the beginning of the second branch is equal to that at the second branch. The same also occurs for the concrete compression force C_{cr} as shown in Figure 2.12. In this figure, the normal force T_{cr} and the shear force V_{dcr} of the longitudinal steel bars (by the cracking of the second branch) are also depicted. By the cracking of the second branch of the critical crack, the stirrups are brought into action. The gradual opening of the second branch, from the tip of the first branch towards the load point, requires a gradual increase of the concrete shear

23

force V_{ccr} at the beginning of the second branch to balance the developed force V_s of stirrups.

Moreover, the opening of the second branch of critical crack causes an increase ΔV_d in the shear force of the longitudinal steel bars. However, it is important to note that its existence is only due to inclusion of stirrups. Thus, the forces acting at failure on the portion of the beam above the critical diagonal crack can be considered to be those shown in Figure 2.13.
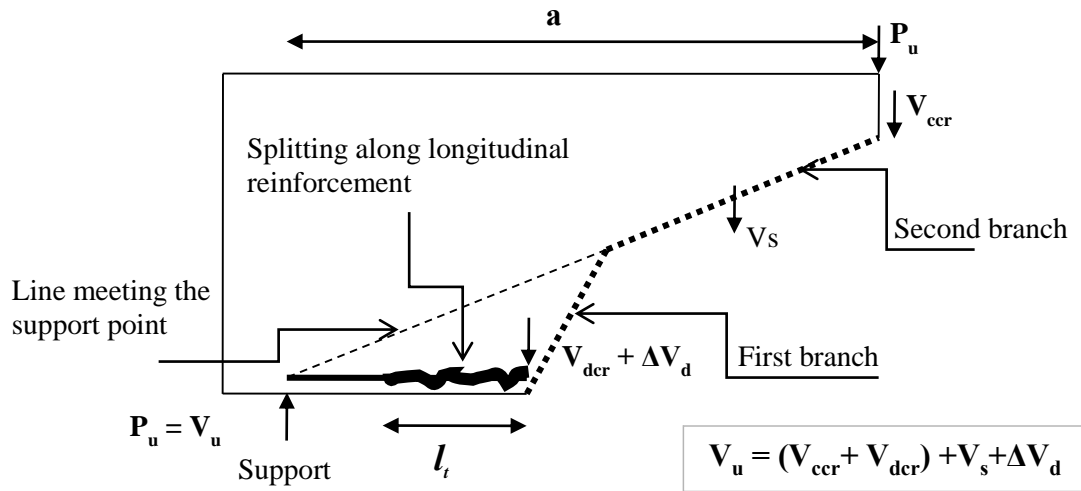
Figure 2-13 : Distribution of forces in beam (based on Zararis theory).

Shear force, V_{cr} at the beginning of cracking of second branch is the sum of the dowel force in longitudinal reinforcement, V_{dcr} and shear force in concrete at the time of cracking, V_{ccr} *i.e.* $V_{cr} = V_{ccr} + V_{dcr}$. Then, through the vertical equilibrium of forces;

$$V_u = V_{cr} + V_s + \Delta V_d \qquad (2.7)$$

Although yielding of stirrups at least at the location of critical crack is an important condition for shear failure, however, mere existence of this condition is not sufficient. The shear failure of a slender beam is caused only when, in addition to the yielding of stirrups, the shear force of longitudinal steel bars, V_d brings about a horizontal splitting of concrete cover along the longitudinal reinforcement. This splitting results in the loss of the shear force V_d and, consequently, the failure of beam. Preventing this splitting hinders the shear failure. It has been assumed that splitting is caused when the tensile stresses developed along the reinforcement in a distance l_t

from the point of initiation of critical crack exceeds the tensile strength, f_t of concrete. Forces acting in the region of horizontal splitting are depicted in Figure 2.14.
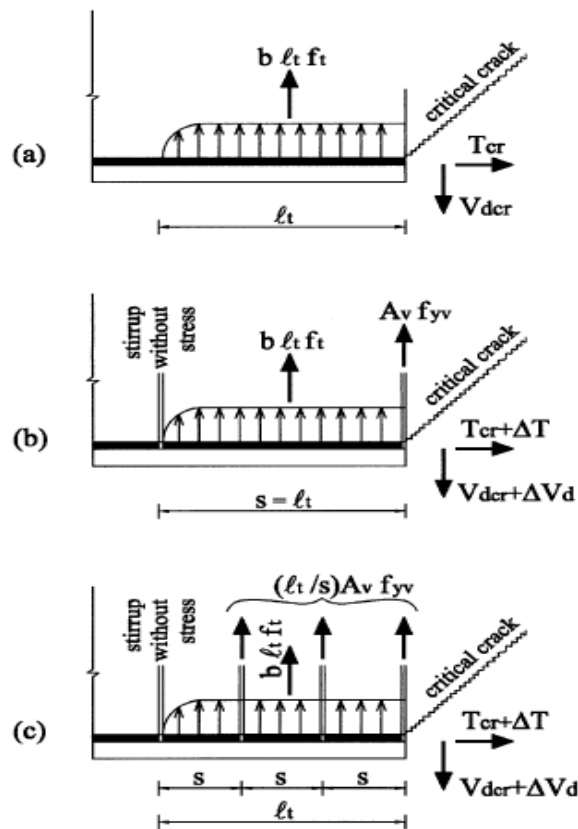
Figure 2-14 : Forces acting in the region of horizontal splitting along the longitudinal reinforcement of beam (a) without stirrups, (b) with stirrups at spacing, s= lt and (c) with s< lt

This splitting length l_t has been believed to have a constant value in any case which is of the order of 0.5d. Taking into account the values for V_{cr}, V_s and ΔV_d, the final equation proposed by Zararis for ultimate shear capacity V_u of beams with stirrups, in its complete form, is as under:-

$$V_u = [(1.2 - 0.2(\frac{a}{d})d)(\frac{c}{d})f_{ct} + (0.5 + 0.25(\frac{a}{d}))\rho_v f_{yv}]bd \qquad (2.8)$$

2.7.3 Minimum Shear Reinforcement

The manner of splitting along the main reinforcement implies a gradual increase in force V_d in longitudinal steel, accompanied by a gradual increase of the force in

stirrup until yielding occurs. The increase in force in longitudinal steel, ΔV_d can be much larger than the one required for yielding of stirrups. This force, surplus to the one required for the onset of yielding of stirrups, is actually responsible for the horizontal splitting. This force was calculated in two different terms i.e. forces acting along the splitting length l_t (equation 2.9), and the distribution of shear stress along main reinforcement and the axial stress of stirrups (equation 2.10)

$$\Delta V_d = 0.5\rho_v f_{yv} bd \tag{2.9}$$

And,

$$\Delta V_d = 0.28(\frac{\rho/\rho_v}{a/d})f_{yv}bd \tag{2.10}$$

The Minimum amount of shear reinforcement commonly corresponds to a value that restrains the growth of inclined cracking, providing an increased ductility and preventing a sudden shear failure. To avoid undesirable widening of the critical diagonal crack (as well as that of the horizontal splitting crack), a surplus of the force ΔV_d must not exist. This occurs when the value of ΔV_d given by Equation 2.9 equals the one given by Equation 2.10. Equating these two equations, the ratio ρ_v of shear reinforcement, in relation to the ratio ρ of main tension reinforcement, must satisfy the following equation:-

$$\frac{\rho}{\rho_v} \leq 1.75(\frac{a}{d}) \tag{2.11}$$

Equation 2.11 constitutes the criterion that the minimum shear reinforcement must fulfill. When the ratio $\rho/\rho_v > 1.75(a/d)$, the shear failure of a beam is accompanied by a quick and extensive splitting crack along the longitudinal reinforcement, as well as by significant widening of the critical crack.

2.8 Modification in Zararis Theory

Zararis considered that the splitting length, l_t has a constant value which is about 0.5d. It is believed that this splitting length is linked with the development length, l_d of the bars. This concept is based on the fact that the factors influencing the development length are similar to those linked with the splitting length along main reinforcement.

Purpose of providing development length is to enable the bars to attain average bond stress over length of embedment so that splitting of highly stressed bars is avoided. According to ACI Code, the development length is influenced by size, location and number of bars, concrete cover, coating on the reinforcement, confining reinforcement, yield strength of steel and compressive strength of concrete. These factors are also thought to be the influencing the splitting length as described above. Therefore, instead of relating splitting length, k with the depth of a beam only, it would be more appropriate to relate it with some fraction of the development length, l_d. Exact value of this fraction may be found by experimental studies, however, for the purpose of this research, it has been assumed that splitting length is 0.25 times the development length for these beams.

By incorporating the above mentioned assumption, Equation 2.9 becomes:-

$$\Delta V_d = 0.25(\frac{l_d}{d})\rho_v f_{yv}bd \qquad (2.12)$$

Now by equating the Equations 2.10 and 2.12, the ratio ρ/ρ_v for minimum shear reinforcement becomes:-

$$\frac{\rho}{\rho_v} \leq 0.89(\frac{l_d}{d})(\frac{a}{d}) \qquad (2.13)$$

Similarly, using the value of splitting length $k = 0.25\ l_d$, the Zararis equation for predicting ultimate shear strength of reinforced concrete slender beams can be modified as under:-

$$V_u = [(1.2-0.2(\frac{a}{d})d)(\frac{c}{d})f_{ct} + 0.25((\frac{l_d}{d})+(\frac{a}{d}))\rho_v f_{yv}]bd \qquad (2.14)$$

2.9 Shear Span

There is no analytical derivation for Shear span yet to be done. There are only three Researchers, who have defined it experimentally or empirically.

- First of all "S. BERNAERT and C. P. SIESS (UUIC, 1955) have suggest that Shear span is equal to 0.11L. They conducted a test series and measured the average distance of first diagonal crack from the support (X_X). First diagonal crack was

assumed to occur at a distance of (a_xL) from the support. At this distance shear strength is Vc', corresponds the shear Vc at the support. By equating these two distance a_x = Xx/L. Graphically shown in fig. 2.15.
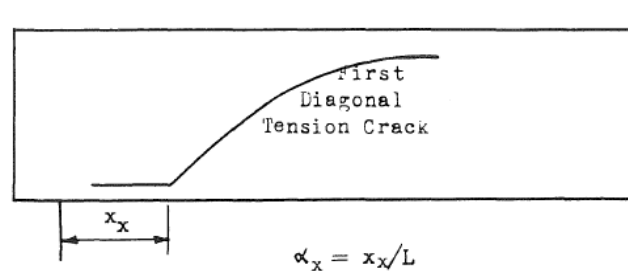
Figure 2-15 : Shear Span (BERNAERT and SIESS)

- "G.N.J. Kani" (U of Toronto, 1966) suggested shear span equal to L/4. He assumed that Max. moment in simply supported beam is equal to shear span times Max Shear fore. Mathematically.

$$M=V*a$$

$$a = \frac{M}{V} = \frac{\frac{wl^2}{8}}{\frac{wl}{2}} = \frac{l}{4}$$

And graphically is shown in fig 2.16.

- Another assumption of Shear Span was made by "P.D. Zarari" (Aristotle University, 2008). He stated that "For slender beam under uniform load, concrete splitting, which results in the formation of second branch of the critical diagonal crack possibly occur at the most stressed area that is the area closest to the support area. For slender beam (a/d >2.5) one can conclude that under a uniform load the ideal shear span is 2.5d.

28
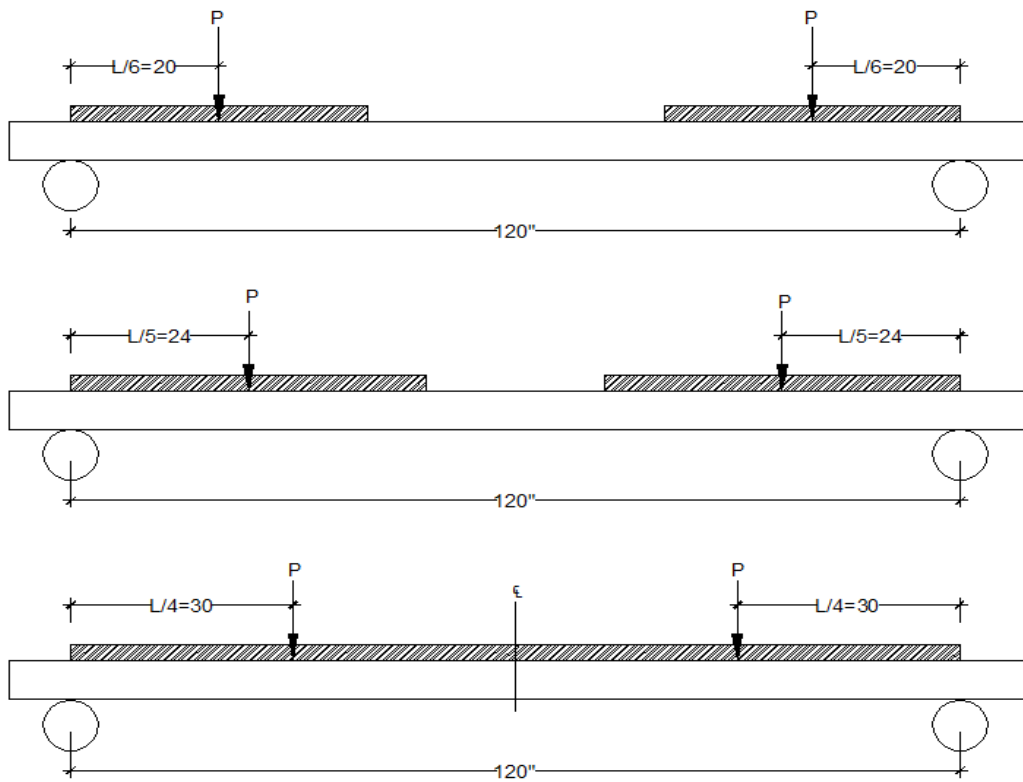
Figure 2-16 : Graphical demonstration of Shear Span (Kani's Theory)

EXPERIMENTAL PROGRAM

3.1. Introduction

A brief on the materials used and experimental / testing procedures followed for the research are summarized in the succeeding paragraphs.

3.2. Mix Design
Keeping in view the member dimensions, Compressive strength of concrete was so selected that minimum shear reinforcement requirement is governed by the empirical equation 2.2 and not by the spacing requirements equation 2.4. In the study, f'c was selected as 4000 psi.

3.3. Materials

3.3.1. Cement
Type I cement conforming to ASTM C 150 - 04 was used. Results of the tests carried out to ascertain the properties of cement are presented in Table 3.1 (Appendix I).

3.3.2. Fine Aggregate
Sand from Qibla Bandi deposit was used. Results of the tests conducted for verification of properties of sand are tabulated in Table 3.2 – Appendix-I. The gradation of the fine aggregate is tabulated in Table 3.3 - Appendix I, and graphically shown in Fig 3.1-Appendix I. Fineness modulus of sand was calculated as 2.45 and specific gravity 2.60.

3.3.3. Coarse Aggregate
Aggregate from Margalla crush site was used in this research. Maximum size for the aggregate was kept as 12.7 mm. For gradation purpose, only three sizes were considered i.e.12.7 mm, 9.5 mm, 4.75 mm. The laboratory test results

are tabulated in Table 3.4- Appendix I. The gradation and sieve analysis was determined in accordance with ASTM C 136 – 01 and tabulated in Table 3.5 - Appendix I, and graphically illustrated in Fig 3.2-Appendix I.

3.3.4. Reinforcing Steel

Reinforcement bars of #8 and #5 sizes were used as longitudinal tensile and compressive reinforcement respectively. #2 and #3 bars were used as transverse reinforcement (Shear Reinforcement). The grade 60 and grade 40 steel was used for longitudinal and transverse reinforcement respectively. Stress-strain diagram (#8 bar) is shown in Fig 3.3-Appendix I.

3.3.5. Superplasticizers

Superplast 470 (product of Ultra Chemical Company), a high performance concrete super plasticizer based on modified poly-carboxylic ether, was used in the research. The dosage was kept constant throughout the research work as 0.9% by weight of cement. The technical data of Superplast 470 is tabulated in Table 3.6 Appendix I.

3.3.6. Water

For mixing and curing of the concrete, potable water was used.

3.4. Casting of Specimens

Specimens were cast as per ASTM C 31 and 31M. Eight beams were prepared with single batch of concrete procured from a batching plant. For determination of the compressive strength of concrete, 12 cylinders (6"x12") were also prepared.

3.5. Description of Specimens

Eight reinforced concrete beams were cast to investigate the shear behavior with various amounts of shear reinforcement. These beams having longitudinal tensile steel reinforcement ratio of 1.48 %, were divided into four series depending upon the amount of shear reinforcement ratio. N - Series did not have any shear reinforcement, whereas

A - Series had minimum amount of shear reinforcement ratio as required by ACI 318 – 08. Z - Series had minimum shear reinforcement as specified by Zararis and mentioned in equation 2.11. M - Series had minimum amount of shear reinforcement as per the Modified Zararis equation as mentioned in equation 2.13. The cross-sectional dimensions of all the eight beams were 10" x 18". The specification of specimens and material properties are shown in Table 3.7 - Appendix I, and diagrammatically illustrated in Figure 4.4 - Appendix II.

3.6.   Fabrication of Specimens

Casting of specimens was done as per ASTM C 31/31M. The specimens were cast in 1" thick plywood shuttering. Shuttering was prepared in such a manner that it could be dismantled easily. The steel reinforcement cage was placed in the formwork over the 1" spacers and tied up with the bars. The concrete for the beams was mixed in a batching plant set up at Zarkon Heights Building, Rawalpindi. The concrete was transported to the casting site through transit mixers and poured manually in the specimens. The formwork was removed from beams after 48 hours. All the beams were cast on 02 Jan, 2015. Hessian cloth was placed on the beams and cured in open whereas; test cylinders were cured in water.

3.7.   Testing of Specimens

3.7.1. Test Setup
The testing facility established at SCEE, NUST was used for this experimental program. The load was applied through a hydraulic jack and pump having 120 tons capacity. The beams were placed on the supports with the help of a fork lifter. The supports comprised of 4" dia solid steel bars, making the beam simply supported at both ends. The load was applied using remote control in increments of 2.5 tons which was displayed at the display panel. Two flat footed rails were used to transfer the load on beam in a uniformly distributed manner as Shown in fig.4.2 and fig 4.3 Appendix II. Three LVDTs were placed under the beam at mid span and at quarter points to measure the deflections at these points. Deflections were measured and recorded

through the Structural load analysis and data logging system. Diagrammatically the test setup is shown in Figures 4.3 (c) Appendix II.

3.7.2. Loading Arrangement

A main challenge in the research was that, How to apply load in a Uniform pattern. The exact distribution of load can only be ensured if the load comes at 45 degree from the load point (Hydraulic Jack). But it is not possible because the clear distance between the beam top and hydraulic jack plunger is 30", While the required is (120/2) 60". So another approach is used, that is the use of a flat footed rail which is very stiff material. Fig .4-3 (A) Appendix II. Later on it was thought that this arrangement does not depicts the true picture of uniform load because the load will distribute in the influence area of plunger only and sides of the beam will remain unloaded. To accommodate this problem it was decided to used two Flat Footed Rail as shown in fig 4-3 (B) Appendix II. Later on a little bit modification was made (round bar by Square bars, Trimming of Rail surface) and the final arrangement used as shown in fig. 4-3(C) Appendix II.

3.7.3. Testing Procedure

The beams were planned to be tested under uniformly distributed loading. The load was applied after centering and aligning the specimens on the test setup and making all necessary arrangements for recording the load and deflection. The load was applied in increments of 2.5 tons, and deflections recorded at each load increment. During the application of load, the cracks were observed and marked on the beams.

EXPERIMENTAL RESULTS

4.1. Concrete Strength

Twelve cylinders were cast in total at the time of pouring of concrete in specimens. Three cylinders each were tested as per ASTM C 39 after 7, 14 and 28 days respectively and the remaining three cylinders were tested on the day of the testing of beams. Testing of cylinder was carried out at Construction Material Laboratory (CWO) Islamabad. The average compressive strength obtained on was 4150 psi.

4.2. Recording of Measurements

4.2.1.1. Deflections

The LVDT"s were used to measure the deflection of beams. Three LVDT"s were placed under the beam and were connected to the computer based structural load analysis and automation system (Made by National Instruments (USA) and assembled locally) shown in Fig. 4.1 Appendix II. The deflections against each load was measured by LVDT"s and automatically stored in computer as a text file by software (Labview) based data acquisition system. The detailed values of deflections against loads are shown in Appendix II.

4.3. Test Behavior of Specimens

Testing of all eight specimens was carried out at NUST Laboratory on 27 May 2015. The samples were loaded in a uniformaly distributed pattern as shown in fig 4.2 Appendix II. Load was applied in increments of 2.5 Tons. After each increment of load, cracks in the beams were observed and marked. Deflections were also noted after each increment of load. Detailed behavior of each specimen is as under:-

4.3.1. Specimen N-1

No cracks were observed till 5 tons load, flexural cracks were observed at 7.5 ton loading at middle span of the beam. Flexural cracks increased both in number as well as in size upto 17.5 tons load. At 20 tons load, inclined cracks appeared near the supports and at 25 tons, large inclined cracks were observed close to the supports. At 33.25 tons load a loud was listen that means the failure of beam because of the inclined cracks. Load deflection data and plots are given in table 4.1 and figure 4.5 respectively (Appendix II). The crack pattern of the beam is shown in the figure 4.6 (Appendix II).

4.3.2. Specimen N-2

Initial flexural cracks appeared at a load of 5 tons. Length of flexural cracks was observed to be increasing at 15 tons and few new flexural cracks near the quarter span appeared at the same load. Inclined cracks near both supports appeared at 20 tons load and kept widening and increasing upto 30 tons. The beam failed at 35.57 tons due to inclined cracks. Load deflection data and plots are given in table 4.2 and figure 4.7 respectively (Appendix II). The crack pattern of the beam is shown in the figure 4.8 (Appendix II).

4.3.3. Specimen A-1

Few flexural cracks of small length started to appear in beam at 10 tons. Number and size of flexural cracks kept increasing up to 17.5 tons. Inclined cracks started to appear at 20 tons load but did not suddenly increase in length like N - Series beams. These inclined cracks increased in length up till 25 tons reaches. At 35 tons, concrete near the left support started to disintegrate and the inclined cracks widened significantly. Widening of cracks kept on increasing till 60 ton of load. The beam failed at 68.56 tons. Load deflection data and plots are given in table 4.3 and figure 4.9 respectively (Appendix II). The crack pattern of the beam is shown in the figure 4.10 (Appendix II).

4.3.4. Specimen A-2

Small flexural cracks close to mid span started appearing at 10 tons and increased slightly in length upto 20 tons. Initially straight cracks near the quarter points started to become inclined at 25 tons. New inclined cracks near both supports emerged at 30 tons load and increased in size. Inclined cracks started getting closer to each other near the supports and finally joined together at 47.5 tons. At same load, width of inclined cracks considerably increased and small concrete particles started spalling off. The beam failed at 65.50 tons due to the inclined cracks. Load deflection data and plots are given in table 4.4 and figure 4.11 respectively (Appendix II). The crack pattern of the beam is shown in the figure 4.12 (Appendix II).

4.3.5. Specimen Z-1

Small flexural cracks started to appear in the middle region of beam at 10 tons. These cracks started to get slightly inclined at 25 tons. Growth of flexural cracks continued upto 30 tons and was slowed down thereafter upto 35 tons and started to further increase in length later on. New inclined cracks appeared after 27.5 tons near the supports and continued to grow towards the supports. Almost all inclined cracks joined together close to the supports at 50 tons. After that, these cracks increased slightly in length but started widening. Flexural cracks increased after 45 tons, reaching almost the 2/3 of the depth of beam. At 55 tons, the concrete near the loading points started to crush and disintegrated at 57.5 tons. Few sounds were also observed from the beam at this load. The beam failed both by crushing of concrete and widening of inclined cracks at 70.43 tons. Load deflection data and plots are given in table 4.5 and figure 4.13 respectively (Appendix II). The crack pattern of the beam is shown in the figure 4.14 (Appendix II).

4.3.6. Specimen Z-2

Small size flexural cracks appeared at 7.5 tons and increased in number upto 15 tons. All cracks remained vertical upto 20 tons and the cracks near the quarter span started to get inclined after that. At 25 tons, new inclined cracks appeared and started to grow towards the loading points. The inclined cracks started to join together close to the

supports at 40 tons. At 37.5 tons, small cracks along the longitudinal reinforcement appeared at the point of initiation of inclined cracks, however, these did not grow further in size till failure. Growth of inclined cracks was reduced after 40 tons and the flexural cracks kept increasing in size. At 52.5 tons, horizontal cracks in concrete near the load points appeared which further increased and caused failure of concrete at 60.20 tons. At the same load, the concrete from the inclined cracks also started to chip off. Load deflection data and plots are given in table 4.6 and figure 4.15 respectively (Appendix II). The crack pattern of the beam is shown in the figure 4.16 (Appendix III).

4.3.7. Specimen M-1

Small flexural cracks started to appear in the middle region of beam at 7.5 tons. These cracks started to get slightly inclined at 20 tons near the quarter spans. Growth of flexural cracks continued up to 27.5 tons. New inclined cracks appeared after 25 tons near the supports and continued to grow towards the supports. Inclined branches from existing cracks also developed at 25 tons. Inclined cracks started getting closer to each other close to supports. The growth was reduced but the widths increased. At 47.5 tons, inclined cracks significantly widened, cracks along the longitudinal reinforcement also appeared and the beam failed at 65.03 tons due to inclined cracks. Load deflection data and plots are given in table 4.7 and figure 4.17 respectively (Appendix II). The crack pattern of the beam is shown in the figure 4.18 and 4.19 (Appendix II).

4.3.8. Specimen M-2

Flexural cracks started appearing at 7.5 tons. All cracks remained vertical up to 17.5 tons and then the cracks near the quarter span started to get inclined. At 20 tons, new inclined cracks appeared and started to grow towards the load point. The inclined cracks started to join together load point and their widths increased and finally beam failed due to these cracks at 64.15 tons., their growth remained slow till 40 tons but width continued to increase. Flexural cracks kept propagating till 42 tons and then stopped. At 45 tons, inclined cracks reached the Load deflection data and plots are

given in table 4.8 and figure 4.21 respectively (Appedix II). Crack pattern of the beam is shown in the figure 4.22 and figure 4.23 (Appendix III).

4.4. Summary of Behavior

Behavior of the beams with load can be described briefly as given below:

- Initial flexural cracks in almost all cases occurred between 7.5 – 10 tons load.

- Existing flexural cracks extended and new flexural cracks appeared in the beam by increasing the load. The flexural cracks in the shear spans started to get inclined above 20 tons in case of samples of Z and M series. Whereas, in A and N series, sudden inclined cracks of large lengths appeared above 22.5 tons.

- The inclination of diagonal cracks was observed to be between 30 and 45 degrees.

- It was observed that two distinct branches of "critical diagonal crack" did not appear in Z and M series. However, inclination of these cracks remained almost constant. Similarly, few cracks along the longitudinal reinforcement did appear in these beams but splitting of concrete did not occur.

- N series beams failed immediately after appearance of sudden diagonal cracks. The same did not happen in A series where diagonal cracks appeared on loading similar to N series, however, their growth remained slow and failed at higher loads.

- In Z series, failure of both beams involved crushing of concrete near load points in addition to splitting of diagonal cracks.

- In some beam, left quarter and right quarter deflections are not exactly similar, this may be due to local non-homogeneity of the section or an error in LVDT's.

ANALYSIS AND INTERPRETATION OF TEST RESULTS

5.1. General

An experimental program was conducted to study the shear behavior of reinforced concrete slender beams having moderate longitudinal reinforcement under uniformly distributed load and to evolve minimum shear reinforcement criteria. Beams were classified into four different categories basing on the minimum amount of shear reinforcement provided according to existing and established guidelines. The influence and effects of the variation in transverse reinforcement was observed from the shear strength, cracking and failure mechanism of these beams. All beams have shown similar pattern as described below:

- In the first stage of testing, all beams behaved elastically, and deflection were proportional to loads before appearance of the flexural crack.

- Redistribution of stresses occurred after cracks result in extra deflections. The deflections remained elastic but load-deflection curve inclining with a lesser slope.

- The flexural cracks remained vertical in mid span region. The cracks near the supports started to incline after they crossed the longitudinal reinforcement.

- The vertical cracks in zero shear region developed rapidly at first. However, their progression reduced and inclined cracks developed more rapidly.

- Diagonal cracking caused sudden failure in N-series beams. The failure was caused due to the excessive widening of a diagonal crack.

- Beams with ACI specified minimum shear reinforcement (A-Series) developed several cracks before failure. Main cause of failure in this series was also the diagonal crack in the beam. Final failure consisted of sudden widening of one major diagonal crack.

- Zarari's specified minimum shear reinforcement beams (Z-series) failure was observed at maximum load. Several cracks appeared before failure. Splitting of concrete was not observed along longitudinal reinforcement and two distinct branches of the critical diagonal crack were also not witnessed.

- MZ-series beams also behaved similar to Z-series beams. However, they failed at comparatively lesser load.

5.2. Load Deflection Response

Load deflection response of eight beams is plotted in figure 5.1 (Appendix III). The deflections at mid span of beams were measured and plotted. The plot indicates that the beams behaved elastically till about 15 kip load. Initial cracks were observed in all beams close to this load. After the crack initiation, the slope of the curves reduced demonstrating the reduction in stiffness of beams because of cracking. It can be seen that the measured deflections of all beam specimens lie below the theoretically calculated cracked and un-cracked sections. Beam without shear reinforcement lie under the line demonstrating lesser flexibility.

5.3. Shear Span for UDL

The definition of shear span for beams under UDL is not very clear. An effort was also made to find it experimentally, by using the results of experimental studies conducted in the department at NUST. The parameters of other beams were same except shear span. It was reasonable to assume that the beams should fail at about same moments irrespective of the loading pattern/mechanism. Equating the moments of two point loading with UDL loading, shear span values for distributed loads were calculated. It was observed that the shear span value is more close to the Kani's expression as explained in Section 2-9. Tabulated data is presented in Table 5.3 (Appendix III).

5.4. Shear Strength Calculation

According to ACI equation, shear strength of beam consists of contribution from concrete and steel. Shear strength provided by steel is determined from ACI Eq. 11.15 which is believed to provide an accurate prediction of shear strength at ultimate loads where lateral steel is assumed to have yielded. Contribution from concrete is

considered by dowel action, aggregate interlock between shear cracks, shear in compression zone and shear span to depth ratio etc. as described in Chapter 2. ACI specified a factor "2" collectively for all these parameters. The equation $Vc = \gamma.\sqrt{f'c}\ bd$ was considered as a general expression. Value of "γ" is calculated and tabulated in Table 5-1. It can be seen that the factor "γ" has larger values than ACI recommended value of 2.

Relationship between transverse reinforcement ratio and shear strength is plotted in figure 5-2. It was observed that shear increases with increase in transverse reinforcement ratio. The presence of stirrups in concrete control crack width, and enhances the shear strength through aggregate interlocking. It also reduces concrete splitting along the longitudinal reinforcement as discussed in literature review.

Fig. 5-3 to Fig. 5-5 (Appendix III) compare the experimental shear strength of the beams tested in this study with the theoretically predicted shear by ACI, Zararis and Modified Zararis equations respectively. It was observed that shear strength predicated by Zararis equation and modified Zararis equation are closer to experimental value than ACI equation.

Shear strength for each series of beams was calculated and predicted according to ACI Equation 11.2, Zararis (Equation 2.8) and the Zararis Equation modified on the concept of development length (Equation 2.14). Experimentally obtained ultimate shear strengths were compared to the theoretical values as illustrated in Table 5-2 and figure 5-6 (Appendix III). This comparison shows that ACI equation gives conservative results. Shear strength calculation by Zararis equation and modified Zararis equation are appropriate in predicting the ultimate shear capacity of beams.

5.5. Moment Capacity of Specimens and Minimum Shear reinforcement.

Nominal moment capacity for the cross-section selected for the specimens was calculated using ACI equation, $Mn = Asfy(d - 0.5a)$. Experimental moment capacities for each beam were calculated by multiplying the ultimate load "Vu" at each loading point with the shear span "a=l/4". Although shear reinforcement is not taken in the flexural design of RC beams. However, it was observed that increase in shear reinforcement, enhances the flexural capacity of the beams because high percentage of stirrups

prevents shear failure increasing ultimate moment. Relationship between ratio of the experimental to theoretical moment capacities and transverse steel ratio is given in figure 5-7 (Appendix III).

It is therefore concluded that there is a minimum amount of shear reinforcement required to achieve the nominal moment capacity predicted by ACI equation. Flexural capacities of N, A, M, and Z-series beams are 52.42%, 102%, 98.40%, and 99.50% of theoretical moment capacity respectively. Figure 5-7 indicates that the value of ρ_v corresponding to 100% flexural capacity is 0.00265. Minimum shear reinforcement required for development of nominal moment capacity can be ascertained by equating the experimental (Vu*a) and theoretical (Asfy (d-0.5a)) moment capacities. The relationship obtained for minimum shear reinforcement ratio is given as under (Derivation is given in Appendix III):-

$$\rho v = \frac{1}{f_{yv}} \left[\frac{f_y \rho}{\left(a/d\right)} \left(1 - \frac{f_y \rho}{1.7\,f'_c}\right) - \gamma \sqrt{f'_c} \right] \qquad (5.1)$$

This equation significantly incorporates all the parameters effecting shear strength of beam and gives quite reasonable value of "ρ_v" when compared with experimental results.

5.6. Modifications to Zararis Equation

In this experimental program, equation developed by Zararis was modified to take into account the effect of development length. It was assumed that splitting length "lt" as shown in figure 2.13, should be equal to some multiple (say α) of the development length "ld" of bars. For this experimental program, value of "α" was assumed to be 0.25 based on a fraction of entire development length. This provided a value of 0.002236 for ρ_v and accordingly the M-Series beams were equipped with this amount of transverse steel. It is believed that minimum shear reinforcement should be such that it should allow the beam to attain 100% of the designed flexural capacity. Figure 5.7 illustrates that for 100% flexural capacity, corresponding value of "ρ_v" is 0.00265. For getting this value of ρ_v from Equation 2.13, the factor α should be taken as 0.99. To keep a safety margin, the factor for development length has been multiplied by

0.9 which reduces it to 0.89 i.e. "lt = 0.89ld". By incorporating this value, equations 2.13 and 2.14 were amended as under:

$$\frac{\rho}{\rho_v} \leq 0.89(\frac{l_d}{d})(\frac{a}{d})$$

(5.2)

$$V_u = [(1.2 - 0.2(\frac{a}{d})d)(\frac{c}{d})f_{ct} + [0.28(\frac{l_d}{d}) + .25(\frac{a}{d})]\rho_v f_{yv}]bd$$

(5.3)

Equations 5.2 and 5.3 mentioned above present the modified form of Zararis' equations and are based on the experimental results. All significant factors contributing to the shear strength of RC beams have been incorporated in these equations.

43

Table 3-1: CEMENT PROPERTIES

Tests	Test results	Specifications
Specific gravity	3.15	ASTM C 188 – 95
Initial setting time	170 minutes at 170C	ASTM C 191 – 01
Final setting time	330 minutes at 170C	ASTM C 191 – 01

Table 3-2 : PROPERTIES OF FINE AGGREGATE

Tests	Test results	Specifications
Specific gravity	2.60	ASTM C 128 – 01
Absorption	1.1%	ASTM C 128 – 01
FM	2.45	ASTM C 33 – 02

Table 3-3: GRADATION OF FINE AGGREGATE

Sieve No	Weight Retained (gm)	Percent Retained	Cumulative Percent Retained	Percent Passing Actual	ASTM C 33 – 02
#4	2	0.2	0.2	99.8	95 – 100
#8	16	1.6	1.8	98.2	80 - 100
#16	134	13.4	15.2	84.8	50 - 85
#30	320	32	47.2	52.8	25 - 60
#50	425	42.5	89.7	10.3	5 - 30
#100	70	7	96.7	3.3	0 - 10
#200	31	3.1	99.8	0.2	
Pan	2	0.2	100	0	

Table 3-4: PROPERTIES OF COARSE AGGREGATE

TEST DETAILS	TEST RESULTS
Impact value (percent)	11.4
Crushing value(percent)	21.4
Abrasion value(percent)	15.8
Specific gravity	2.60

Table 3-5: COARSE AGGREGATE GRADATION

Sieve Size (mm)	Weight Retained (gm)	Percent Retained	Cumulative Percent Retained	Percent Passing	
				Actual	ASTM C 33 - 02
19	0	0	0	100	100
12.5	78	7.8	7.8	92.2	90 - 100
9.5	410	41	48.8	51.2	40 - 70
4.75	488	48.8	97.6	2.4	0 - 15
2.36	24	2.4	100	0	0 - 5

Table 3-6: HIGH RANGE WATER REDUCING AGENT. (TECHNICAL DATA)

DESCRIPTION	DETAILS
Name	Ultra Superplast 470
Form	Viscous liquid
Color	Brown
Specific gravity	1.190 at 20^0C
Alkali content (%)	Typically less than 72.0 g
Chloride content (%)	Nil to BS 5075
Air Entrainment	Less than 2%

Table 3-7: SPECIMEN DETAILS AND MATERIAL PROPERTIES

Beams	f'_c (psi)	Longitudinal tensile bars			Shear steel bars			a/d	d (in)	b (in)
		No	ρ_l(%)	f_{yl} (ksi)	No	ρ_v(%)	f_{yt} (ksi)			
N - Series										
N1	4000	3 # 8	1.48	60	-	-	-	-	16	10
N2	4000	3 # 8	1.48	60	-	-	-	-	16	10
A – Series										
A1	4000	3 # 8	1.48	60	# 2 @ 7.5"	0.13	40	-	16	10
A2	4000	3 # 8	1.48	60	# 2 @ 7.5"	0.13	40	-	16	10
Z – Series										
Z1	4000	3 # 8	1.48	60	# 3 @ 6.5"	0.34	40	-	16	10
Z2	4000	3 # 8	1.48	60	# 3 @ 6.5"	0.34	40	-	16	10
M – Series										
M1	4000	3 # 8	1.48	60	# 2 @ 4.5"	0.21	40	-	16	10
M2	4000	3 # 8	1.48	60	# 2 @ 4.5"	0.21	40	-	16	10
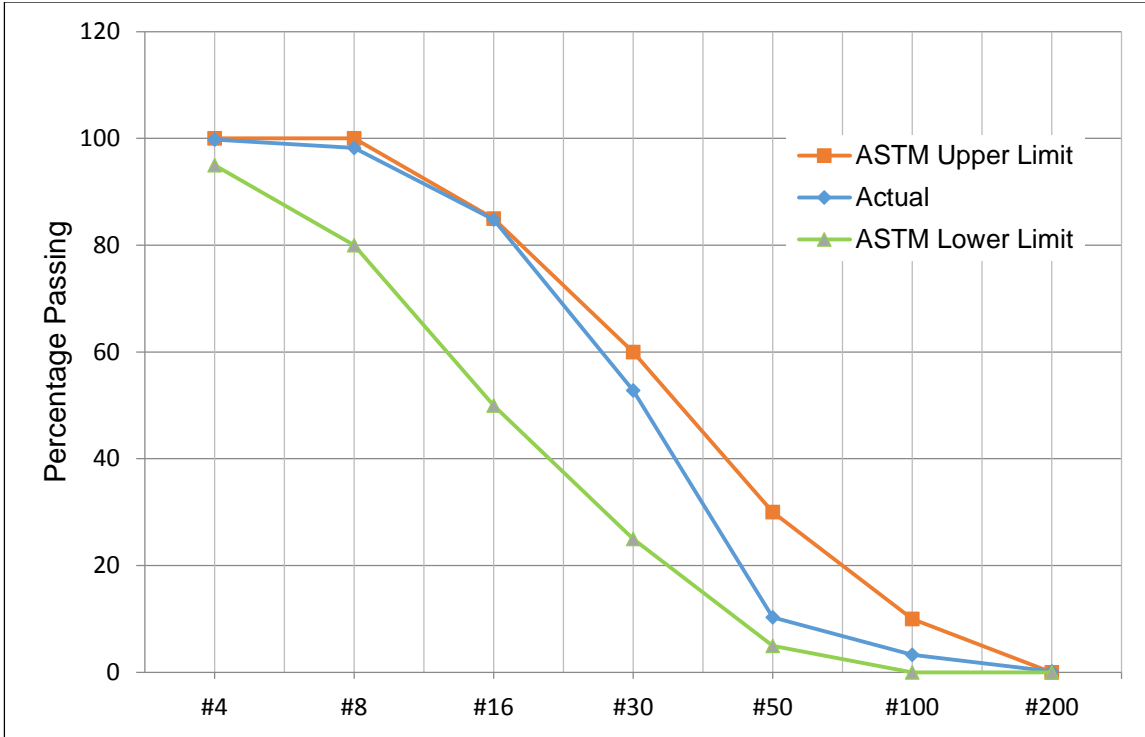
Figure 3-1 : Gradation of Fine Aggregates
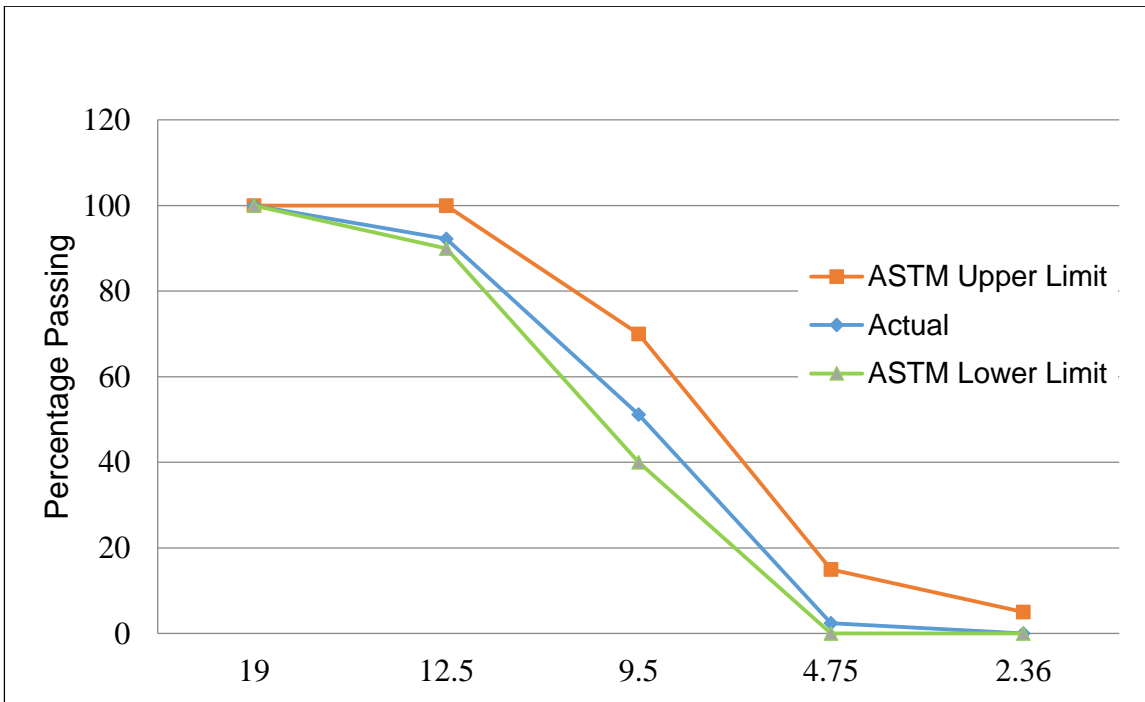
Figure 3-2: Gradation of Coarse Aggregates
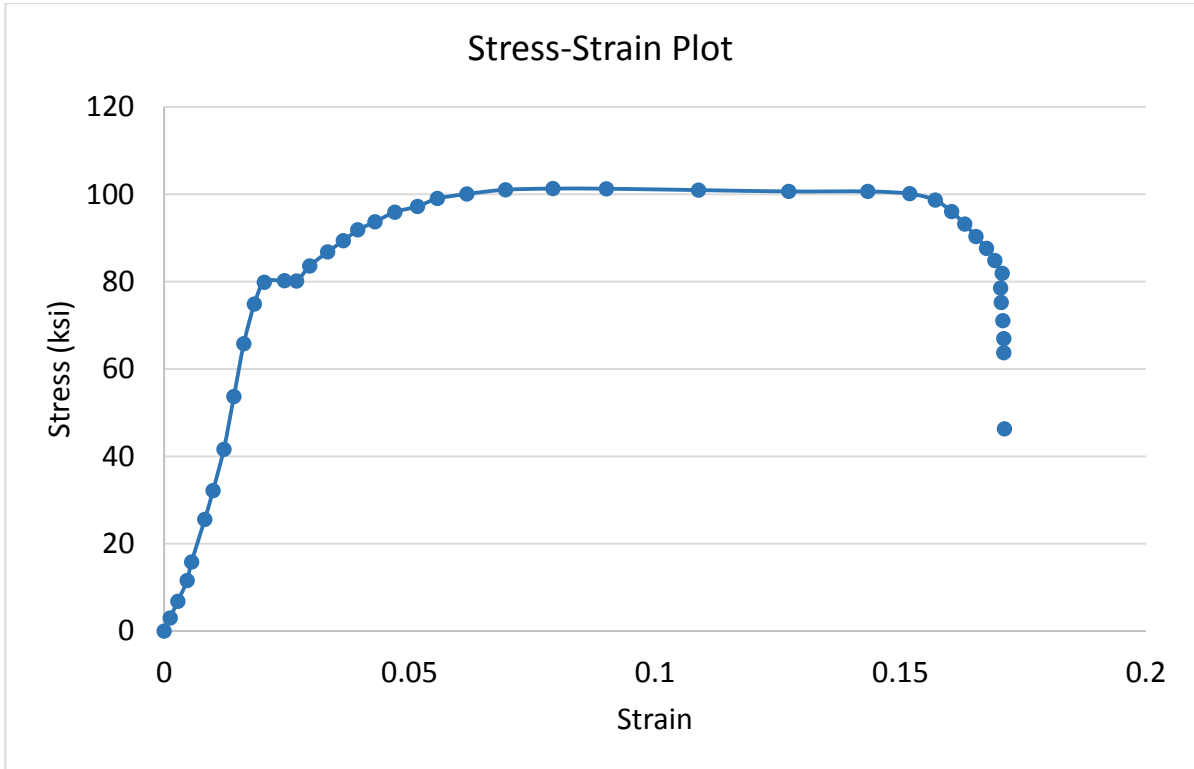
Figure 3-3 : Stress-Strain Relationship of Longitudinal bar

Figure 4.1: Structural Load Analysis and Automation System

Figure 4.2: Load Setup

Figure 4.3: Load Setup
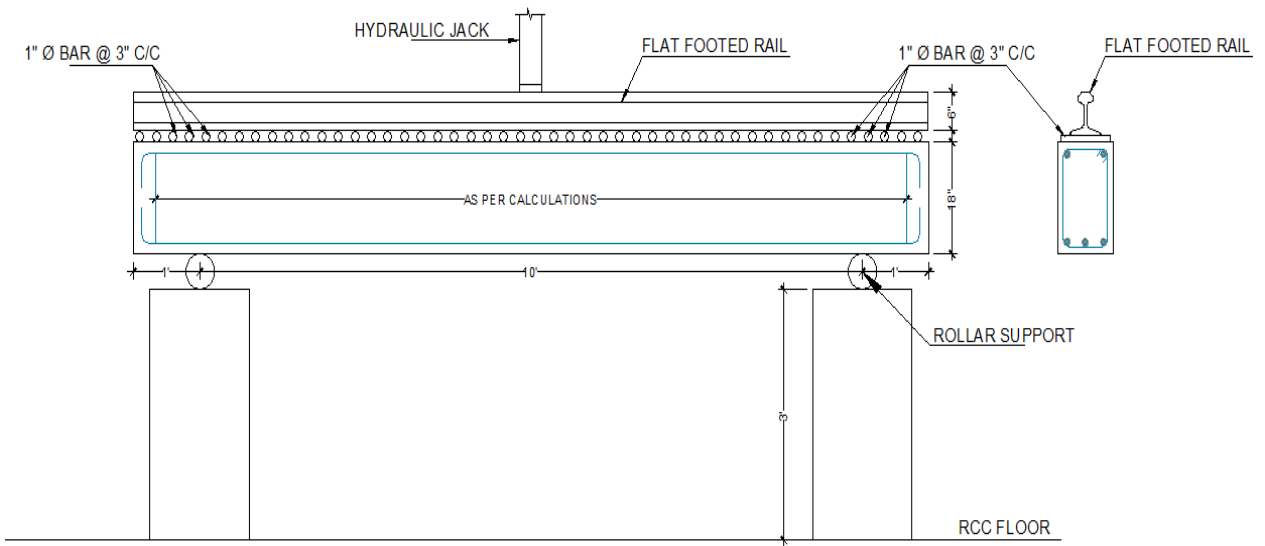
Figure 4.3 (A): Loading Arrangement
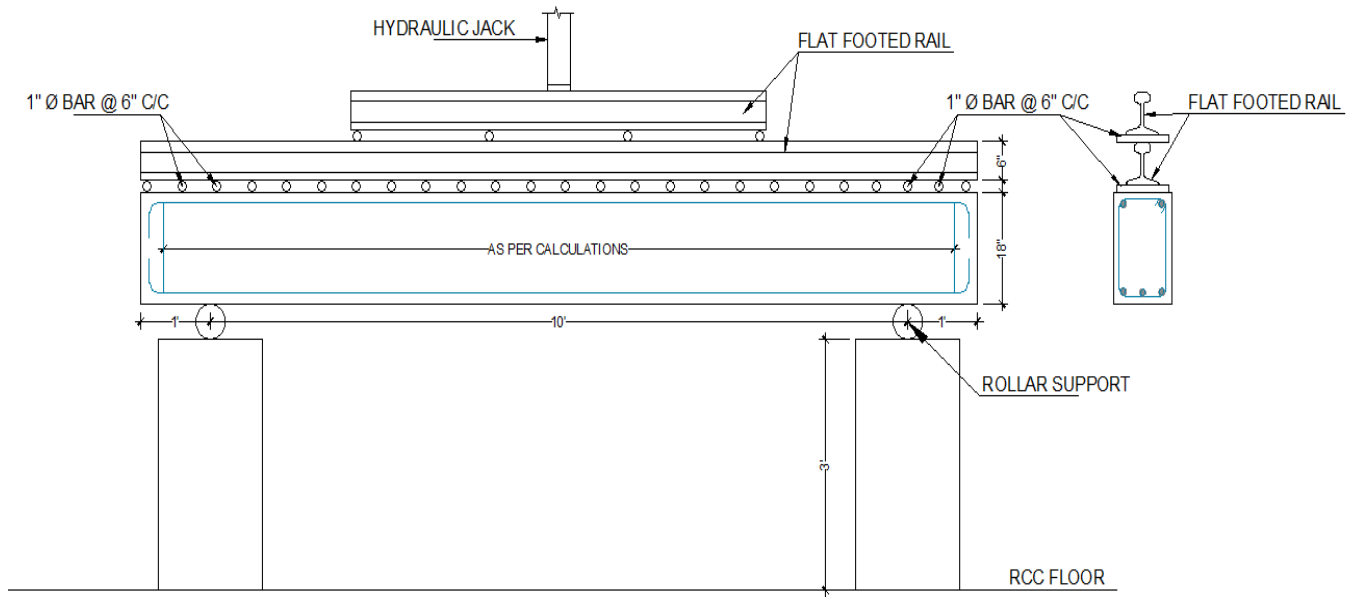
Figure 4.3(B): Loading Arrangement
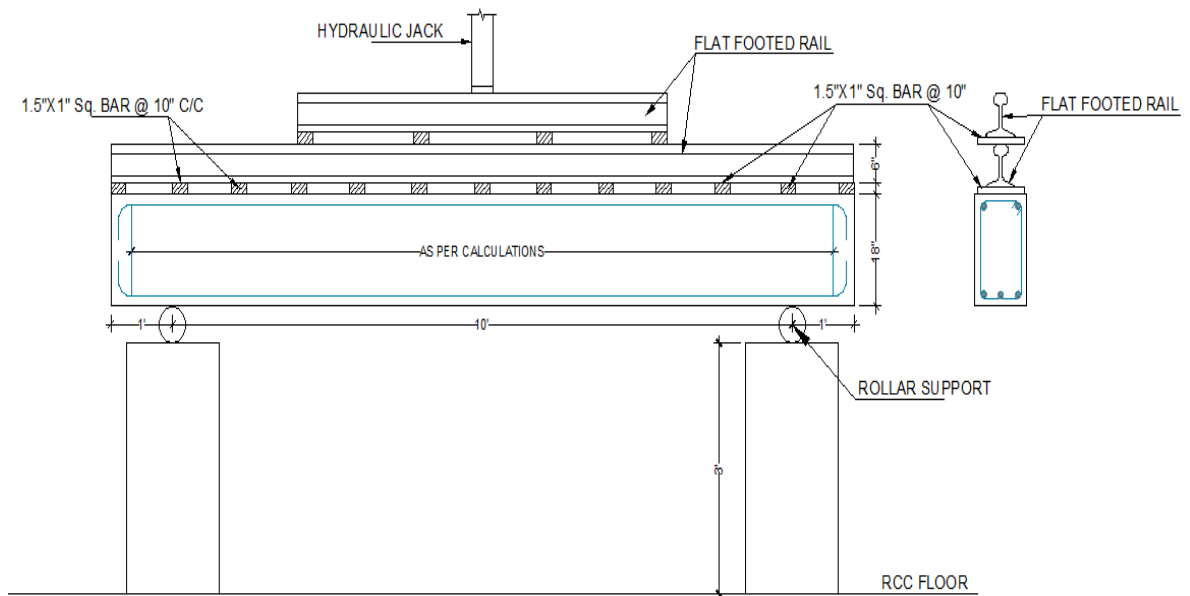
Figure 4.3 (C): Loading Arrangement

51
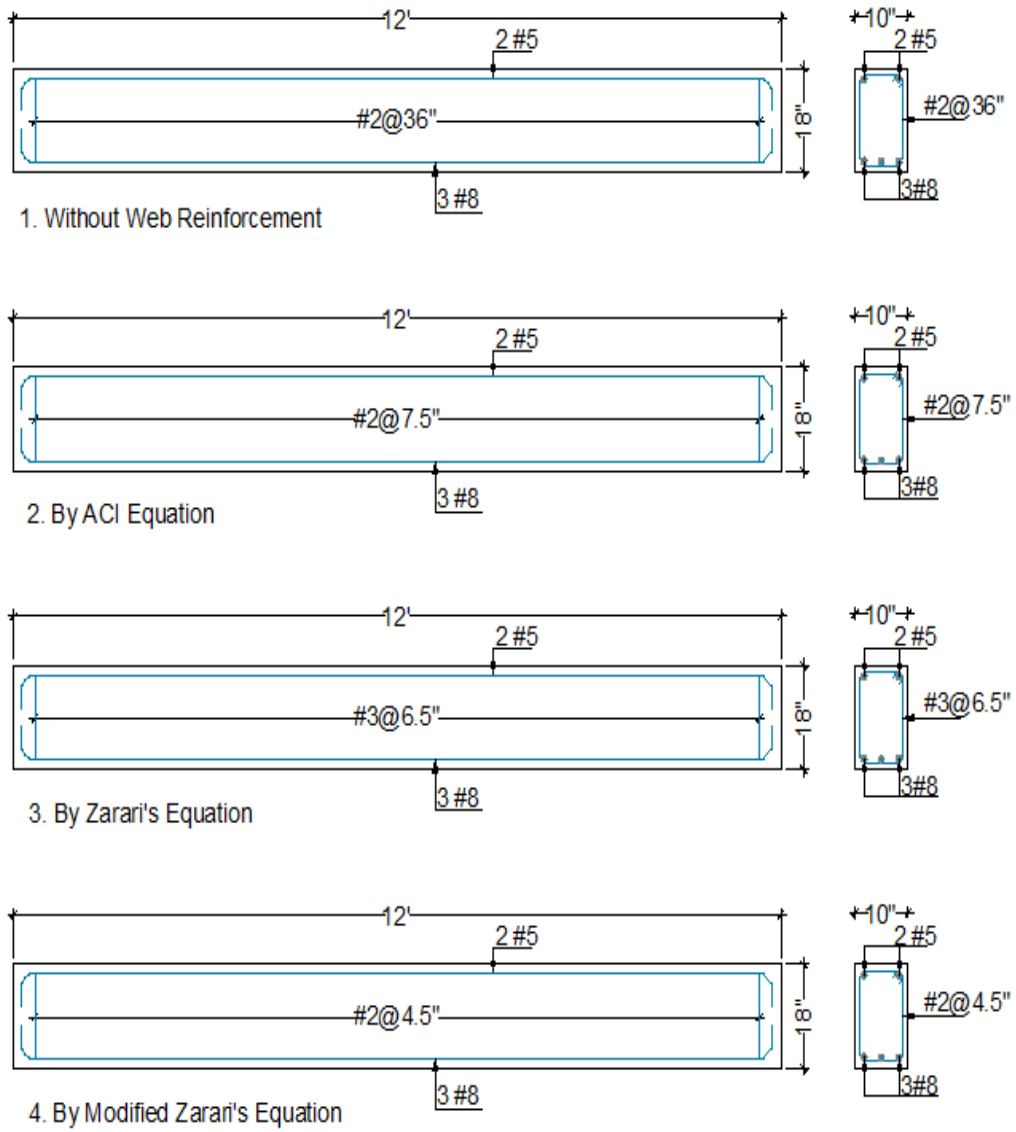
Figure 4.4: Beam Reinforcement

Table 4. 1: Load Deflection Data of Beam N-I

Load Cell		Deflections					
		Left Quarter		Center Point		Right Quarter	
Tons	Kips	mm	Inch	mm	Inch	mm	Inch
0.00	0.00	0.00	0.00	0.00	0.00	0.00	0.00
2.62	5.77	0.37	0.01	0.50	0.02	0.28	0.01
4.95	10.91	0.71	0.03	0.97	0.04	0.50	0.02
7.44	16.40	1.10	0.04	1.50	0.06	0.77	0.03
10.20	22.48	2.05	0.08	2.50	0.10	1.44	0.06
12.52	27.59	2.39	0.09	3.01	0.12	1.70	0.07
15.08	33.24	2.95	0.12	4.01	0.16	2.13	0.08
17.62	38.83	3.35	0.13	4.47	0.18	2.50	0.10
20.32	44.79	4.80	0.19	6.21	0.24	3.02	0.12
22.50	49.59	5.50	0.22	7.30	0.29	3.58	0.14
25.12	55.36	6.25	0.25	8.50	0.33	4.12	0.16
27.54	60.70	7.25	0.29	9.39	0.37	4.55	0.18
30.22	66.60	8.89	0.35	10.54	0.42	5.02	0.20
33.25	73.28	10.72	0.42	11.33	0.45	6.34	0.25
31.26	68.90	11.01	0.43	11.60	0.46	6.68	0.26
27.95	61.60	10.77	0.42	11.31	0.45	6.51	0.26
25.13	55.39	10.63	0.42	11.14	0.44	6.39	0.25
22.63	49.88	10.23	0.40	10.63	0.42	6.07	0.24
20.49	45.16	9.76	0.38	10.04	0.40	5.71	0.22
17.52	38.61	9.21	0.36	9.36	0.37	5.30	0.21
15.02	33.10	8.77	0.35	8.82	0.35	4.96	0.20
12.64	27.86	8.32	0.33	8.26	0.33	4.62	0.18
10.21	22.50	7.88	0.31	7.72	0.30	4.29	0.17
7.74	17.06	7.31	0.29	7.03	0.28	3.88	0.15
5.12	11.28	6.45	0.25	6.01	0.24	3.26	0.13
2.53	5.58	5.68	0.22	5.14	0.20	2.75	0.11
0.00	0.00	4.72	0.19	4.05	0.16	2.06	0.08
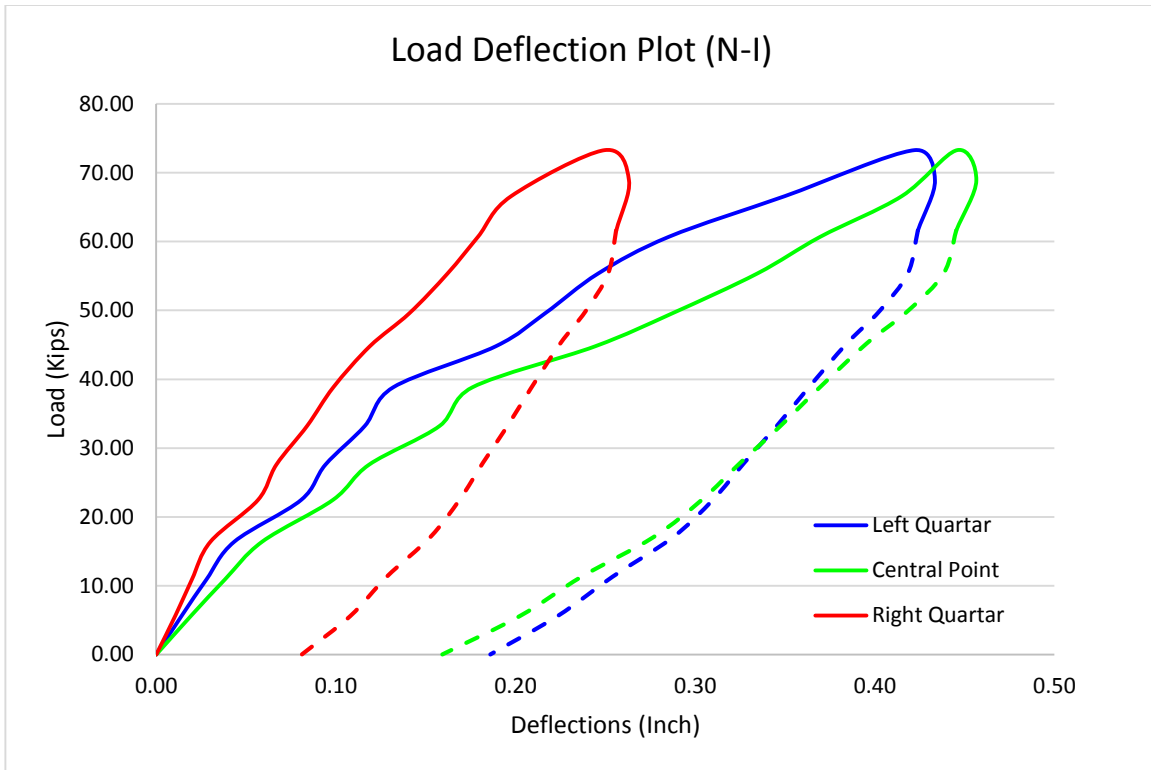
Figure 4-5: Load Deflection Plot of N-I

Figure 4-6: Cracked Pattern of N-I

Table 4.2 Load Deflection Data of Beam N-II

Load Cell		Deflections					
		Left Quarter		Central Point		Right Quarter	
Tons	Kips	mm	Inch	mm	Inch	mm	Inch
0.00	0.00	0.00	0.00	0.00	0.00	0.00	0.00
2.54	5.59	0.02	0.00	0.32	0.01	0.09	0.00
5.15	11.35	0.39	0.02	0.74	0.03	0.19	0.01
7.24	15.96	0.81	0.03	1.26	0.05	0.40	0.02
9.80	21.61	1.23	0.05	1.81	0.07	0.60	0.02
13.31	29.34	1.95	0.08	2.74	0.11	0.80	0.03
16.09	35.47	2.48	0.10	3.45	0.14	1.10	0.04
17.41	38.37	2.77	0.11	3.82	0.15	1.30	0.05
19.98	44.03	3.34	0.13	4.57	0.18	1.70	0.07
23.32	51.39	4.21	0.17	5.67	0.22	1.99	0.08
25.10	55.32	4.84	0.19	6.49	0.26	2.30	0.09
27.92	61.53	5.45	0.21	7.27	0.29	2.75	0.11
29.97	66.06	5.97	0.23	7.93	0.31	3.50	0.14
32.12	70.80	6.82	0.27	8.93	0.35	4.02	0.16
35.57	78.41	11.14	0.44	13.65	0.54	6.88	0.27
30.41	67.01	10.45	0.41	12.74	0.50	6.31	0.25
26.58	58.58	9.90	0.39	12.04	0.47	5.86	0.23
24.83	54.72	9.61	0.38	11.65	0.46	5.61	0.22
23.01	50.71	9.31	0.37	11.25	0.44	5.36	0.21
19.87	43.79	8.69	0.34	10.41	0.41	4.83	0.19
17.86	39.37	8.24	0.32	9.81	0.39	4.45	0.18
14.38	31.69	7.41	0.29	8.73	0.34	3.78	0.15
12.63	27.85	6.99	0.28	8.18	0.32	3.43	0.14
9.48	20.89	6.27	0.25	7.19	0.28	2.82	0.11
6.83	15.06	5.63	0.22	6.36	0.25	2.32	0.09
5.73	12.62	5.39	0.21	6.03	0.24	2.12	0.08
2.77	6.10	4.82	0.19	5.31	0.21	1.72	0.07
0.00	0.00	3.77	0.15	4.18	0.16	1.26	0.05
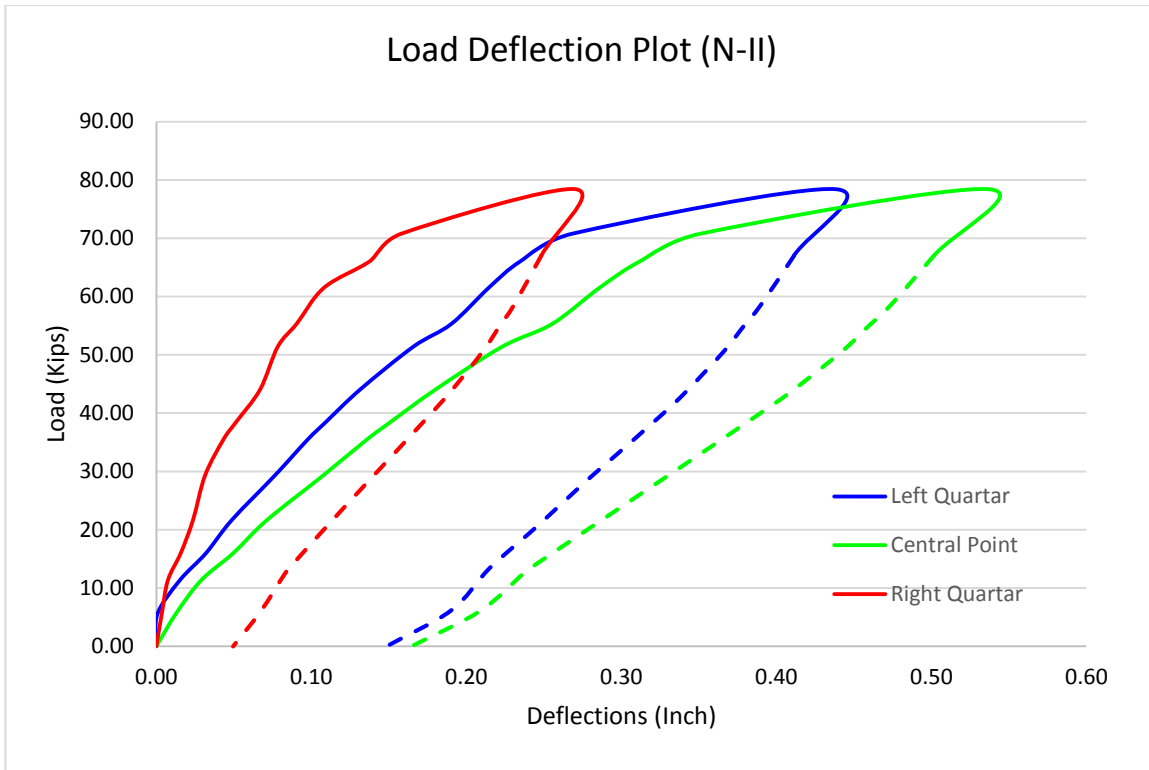
Figure 4-7: Load Deflection Plot of N-I

Figure 4-8: Cracked Pattern of N-II

Table 4.3 Load Deflection Data of Beam ACI-I

Load Cell		Deflections					
		Left Quarter		Central Point		Right Quarter	
(Tons)	(Kips)	mm	inch	mm	inch	mm	inch
0.00	0.00	0.00	0.00	0.00	0.00	0.00	0.00
2.50	5.51	0.30	0.01	0.33	0.01	0.07	0.00
5.19	11.44	0.60	0.02	0.69	0.03	0.27	0.01
7.73	17.05	0.82	0.03	1.13	0.04	0.43	0.02

10.12	22.30	1.14	0.04	1.61	0.06	0.69	0.03
12.50	27.55	1.58	0.06	2.14	0.08	0.94	0.04
15.00	33.06	2.05	0.08	2.67	0.11	1.35	0.05
17.40	38.35	2.48	0.10	3.27	0.13	1.69	0.07
20.00	44.08	2.86	0.11	3.92	0.15	2.00	0.08
22.50	49.59	3.32	0.13	4.51	0.18	2.40	0.09
24.89	54.86	3.91	0.15	5.18	0.20	2.73	0.11
27.50	60.61	4.45	0.18	5.83	0.23	3.14	0.12
30.00	66.12	5.04	0.20	6.40	0.25	3.61	0.14
32.22	71.01	5.72	0.23	7.14	0.28	4.03	0.16
34.50	76.04	6.33	0.25	7.78	0.31	4.46	0.18
37.50	82.65	7.03	0.28	8.57	0.34	4.92	0.19
40.00	88.16	7.68	0.30	9.25	0.36	5.63	0.22
42.50	93.67	8.44	0.33	10.04	0.40	6.24	0.25
45.00	99.18	9.20	0.36	10.89	0.43	6.99	0.28
47.50	104.69	10.18	0.40	12.05	0.47	7.72	0.30
50.00	110.20	11.31	0.45	14.47	0.57	8.74	0.34
52.50	115.71	12.43	0.49	15.96	0.63	9.98	0.39
55.00	121.22	13.94	0.55	18.00	0.71	11.25	0.44
57.50	126.73	15.33	0.60	20.36	0.80	12.30	0.48
60.00	132.24	16.89	0.66	22.53	0.89	13.01	0.51
62.45	137.64	18.53	0.73	24.00	0.94	14.16	0.56
65.00	143.26	20.27	0.80	24.59	0.97	15.90	0.63
65.38	144.09	22.42	0.88	27.08	1.07	17.76	0.70
68.56	151.11	25.98	1.02	31.76	1.25	20.06	0.79
63.49	139.92	26.83	1.06	32.69	1.29	21.99	0.87
60.00	132.24	27.31	1.08	32.16	1.27	22.92	0.90
57.50	126.73	27.39	1.08	31.57	1.24	23.02	0.91
55.00	121.22	27.17	1.07	31.14	1.23	22.36	0.88
52.42	115.53	26.88	1.06	30.53	1.20	21.55	0.85
50.12	110.46	26.45	1.04	30.11	1.19	20.94	0.82
47.50	104.69	25.88	1.02	29.61	1.17	19.87	0.78
45.00	99.18	25.44	1.00	29.06	1.14	19.06	0.75
40.83	89.99	25.11	0.99	28.36	1.12	18.08	0.71
38.66	85.20	24.58	0.97	27.86	1.10	17.34	0.68
33.85	74.61	23.49	0.92	26.84	1.06	16.35	0.64
29.03	63.99	22.92	0.90	25.67	1.01	14.96	0.59
24.14	53.21	21.39	0.84	24.42	0.96	13.41	0.53
19.20	42.31	19.85	0.78	22.79	0.90	12.52	0.49
16.18	35.65	18.00	0.71	21.73	0.86	11.51	0.45
13.92	30.67	16.21	0.64	20.89	0.82	10.00	0.39

| 11.30	24.91	15.00	0.59	19.89	0.78	8.89	0.35
6.41	14.13	13.80	0.54	17.93	0.71	7.37	0.29
1.85	4.09	12.21	0.48	15.81	0.62	5.77	0.23
0.00	0.00	11.18	0.44	15.04	0.59	5.33	0.21
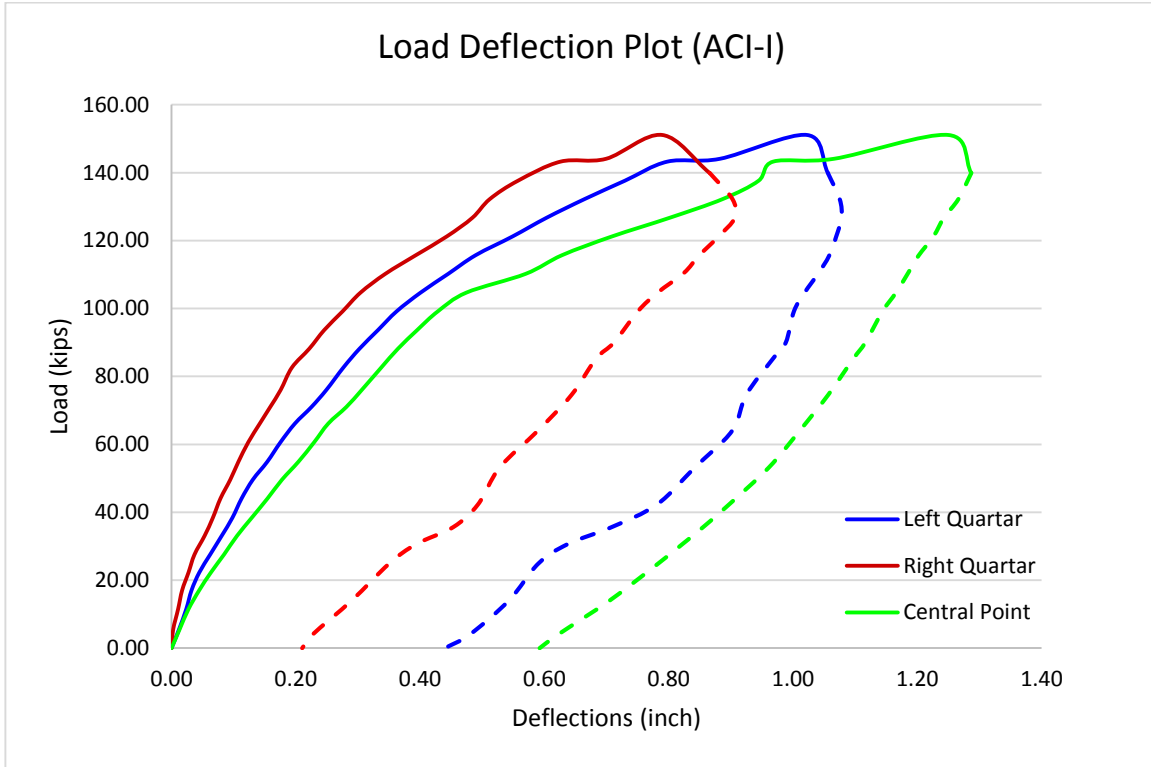
Figure 4-9: Load Deflection Plot of ACI-I

Figure 4-10: Cracked Pattern of ACI-I

Table 4.4 Load Deflection Data of Beam ACI-II

Load Cell		Deflections					
		Left Quarter		Center Point		Right Quarter	
(Tons)	(Kips)	mm	Inch	mm	Inch	mm	Inch
0.00	0.00	0.00	0.00	0.00	0.00	0.00	0.00
2.52	5.55	0.25	0.01	0.53	0.02	0.25	0.01
4.95	10.91	0.45	0.02	0.94	0.04	0.43	0.02
7.40	16.31	0.78	0.03	1.46	0.06	0.55	0.02
10.12	22.30	1.21	0.05	2.07	0.08	0.68	0.03
12.43	27.40	1.60	0.06	2.80	0.11	0.93	0.04
15.21	33.51	2.22	0.09	3.53	0.14	1.24	0.05
17.43	38.42	2.69	0.11	4.14	0.16	1.52	0.06
20.00	44.08	3.34	0.13	4.92	0.19	1.82	0.07
22.61	49.83	3.90	0.15	5.69	0.22	2.21	0.09
25.11	55.34	4.68	0.18	6.63	0.26	2.65	0.10
27.50	60.61	5.29	0.21	7.46	0.29	3.05	0.12
30.22	66.60	6.01	0.24	8.39	0.33	3.51	0.14
32.50	71.63	6.65	0.26	9.31	0.37	3.97	0.16
35.00	77.14	7.51	0.30	10.14	0.40	4.50	0.18
37.50	82.65	8.11	0.32	11.05	0.43	5.10	0.20
40.88	90.10	9.07	0.36	12.13	0.48	5.78	0.23
42.52	93.71	9.83	0.39	13.17	0.52	6.55	0.26
45.14	99.49	10.73	0.42	14.17	0.56	7.38	0.29
47.45	104.58	11.56	0.46	15.40	0.61	8.02	0.32
50.22	110.68	12.67	0.50	16.53	0.65	8.98	0.35
52.50	115.71	13.55	0.53	17.82	0.70	9.90	0.39
55.89	123.19	14.66	0.58	19.05	0.75	10.82	0.43
57.61	126.97	15.72	0.62	20.30	0.80	11.84	0.47
60.66	133.69	16.93	0.67	21.85	0.86	13.15	0.52
62.54	137.84	19.61	0.77	23.59	0.93	15.01	0.59
65.50	144.36	21.64	0.85	25.76	1.01	17.81	0.70
65.29	143.91	22.70	0.89	27.67	1.09	19.50	0.77
61.88	136.38	23.57	0.93	28.01	1.10	20.12	0.79
60.16	132.60	22.85	0.90	27.75	1.09	20.34	0.80
55.38	122.06	22.34	0.88	27.07	1.07	20.27	0.80
50.25	110.76	21.60	0.85	26.36	1.04	19.88	0.78
45.21	99.65	20.74	0.82	25.53	1.01	19.25	0.76
40.32	88.87	19.77	0.78	24.50	0.96	18.48	0.73
35.17	77.53	18.62	0.73	23.24	0.92	17.41	0.69

| 30.43	67.07	17.62	0.69	21.95	0.86	16.27	0.64
25.35	55.88	16.42	0.65	20.56	0.81	15.13	0.60
20.19	44.50	15.21	0.60	19.15	0.75	13.86	0.55
15.19	33.47	13.76	0.54	17.78	0.70	12.56	0.49
10.19	22.45	12.16	0.48	16.44	0.65	10.93	0.43
4.95	10.90	10.83	0.43	14.77	0.58	9.30	0.37
0.00	0.00	8.91	0.35	13.05	0.51	7.46	0.29
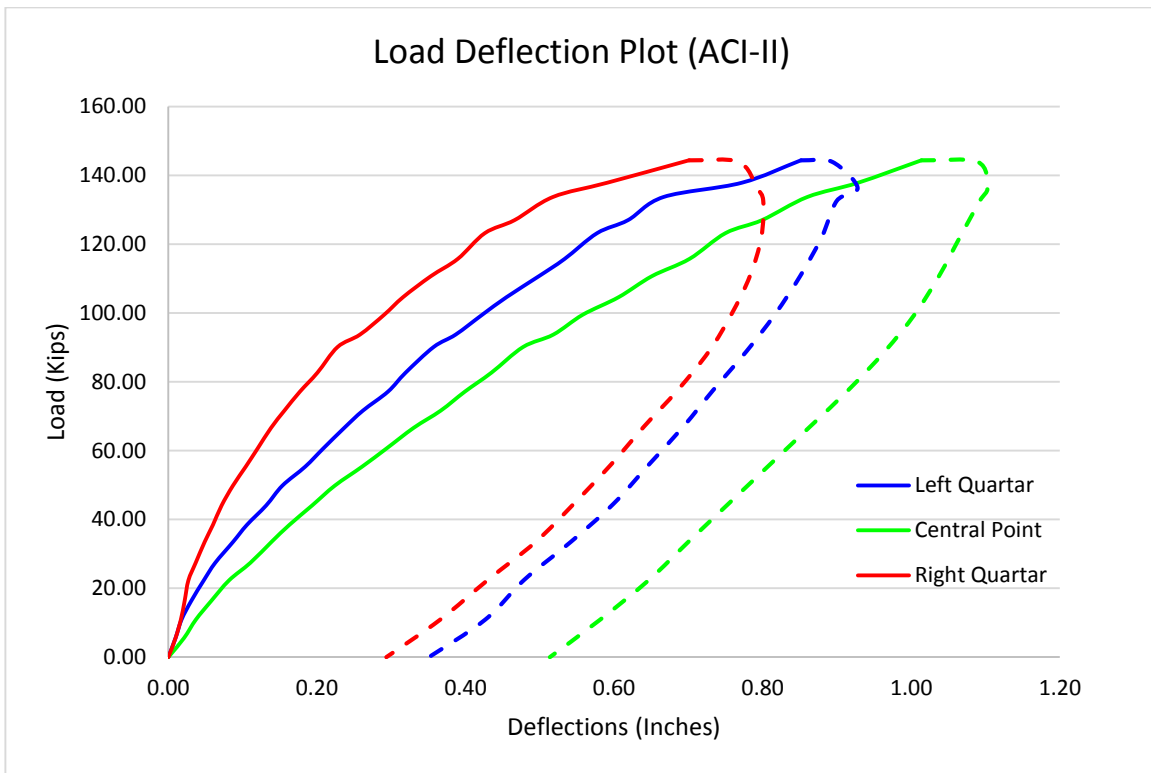
Figure 4-11: Load Deflection Plot of ACI-II

Figure 4-12: Cracked Pattern of ACI-II

Table 4.5 Load Deflection Data of Beam Zarari's-I

Load Cell		Deflections					
		Left Quarter		Central Point		Right Quarter	
Tons	(Kips)	mm	Inch	mm	Inch	mm	Inch
0.00	0.00	0.00	0.00	0.00	0.00	0.00	0.00
2.51	5.53	0.48	0.02	0.46	0.02	0.10	0.00
5.02	11.06	0.98	0.04	1.09	0.04	0.20	0.01
6.89	15.19	1.51	0.06	1.82	0.07	0.32	0.01
10.51	23.17	2.70	0.11	3.40	0.13	0.60	0.02
12.84	28.30	3.12	0.12	3.98	0.16	0.73	0.03
15.29	33.70	3.71	0.15	4.77	0.19	0.91	0.04
17.74	39.11	4.39	0.17	5.70	0.22	1.21	0.05
20.48	45.14	4.88	0.19	6.36	0.25	1.44	0.06
22.11	48.72	5.46	0.21	7.13	0.28	1.79	0.07
24.84	54.75	5.88	0.23	7.74	0.30	2.07	0.08
30.55	67.34	7.44	0.29	9.84	0.39	3.13	0.12
32.05	70.64	7.65	0.30	10.10	0.40	3.27	0.13
35.82	78.94	8.32	0.33	10.96	0.43	3.74	0.15
37.05	81.65	8.82	0.35	11.59	0.46	4.11	0.16
40.68	89.65	9.30	0.37	12.39	0.49	4.57	0.18
42.33	93.30	9.83	0.39	13.06	0.51	4.97	0.20
45.02	99.22	10.52	0.41	13.94	0.55	5.45	0.21
47.75	105.23	11.57	0.46	15.38	0.61	6.20	0.24
50.11	110.44	13.00	0.51	17.76	0.70	7.26	0.29
52.57	115.85	13.65	0.54	18.77	0.74	7.75	0.31
55.00	121.22	15.59	0.61	22.07	0.87	9.29	0.37
57.25	126.19	16.20	0.64	22.87	0.90	9.71	0.38
60.78	133.96	18.50	0.73	26.39	1.04	11.30	0.44
62.35	137.42	18.81	0.74	26.76	1.05	11.51	0.45
65.05	143.36	19.86	0.78	28.29	1.11	12.24	0.48
67.80	149.44	21.36	0.84	30.77	1.21	13.43	0.53
70.43	155.23	22.37	0.88	32.19	1.27	14.13	0.56
68.91	151.88	22.68	0.89	32.85	1.29	14.30	0.56
66.23	145.97	22.45	0.88	32.63	1.28	14.15	0.56
62.51	137.77	21.97	0.86	32.08	1.26	13.82	0.54
60.80	133.99	21.95	0.86	32.06	1.26	13.80	0.54
57.23	126.13	21.60	0.85	31.63	1.25	13.57	0.53

|							
51.64	113.82	20.99	0.83	30.85	1.21	13.14	0.52
49.23	108.49	20.71	0.82	30.50	1.20	12.95	0.51
42.97	94.71	19.90	0.78	29.47	1.16	12.39	0.49
38.88	85.68	19.29	0.76	28.68	1.13	11.96	0.47
34.60	76.25	18.60	0.73	27.77	1.09	11.46	0.45
31.01	68.34	17.92	0.71	26.86	1.06	10.95	0.43
27.60	60.83	17.26	0.68	25.98	1.02	10.47	0.41
25.66	56.55	16.89	0.67	25.50	1.00	10.20	0.40
23.09	50.89	16.38	0.64	24.80	0.98	9.81	0.39
19.81	43.67	15.68	0.62	23.88	0.94	9.29	0.37
17.99	39.64	15.31	0.60	23.39	0.92	9.01	0.35
15.12	33.33	14.72	0.58	22.57	0.89	8.54	0.34
12.68	27.94	14.15	0.56	21.81	0.86	8.11	0.32
7.65	16.87	13.02	0.51	20.27	0.80	7.24	0.29
5.34	11.76	12.59	0.50	19.70	0.78	6.87	0.27
2.51	5.52	12.15	0.48	19.05	0.75	6.42	0.25
0.00	0.00	11.77	0.46	18.47	0.73	6.00	0.24

Load Deflection Plot (Zarari-I)
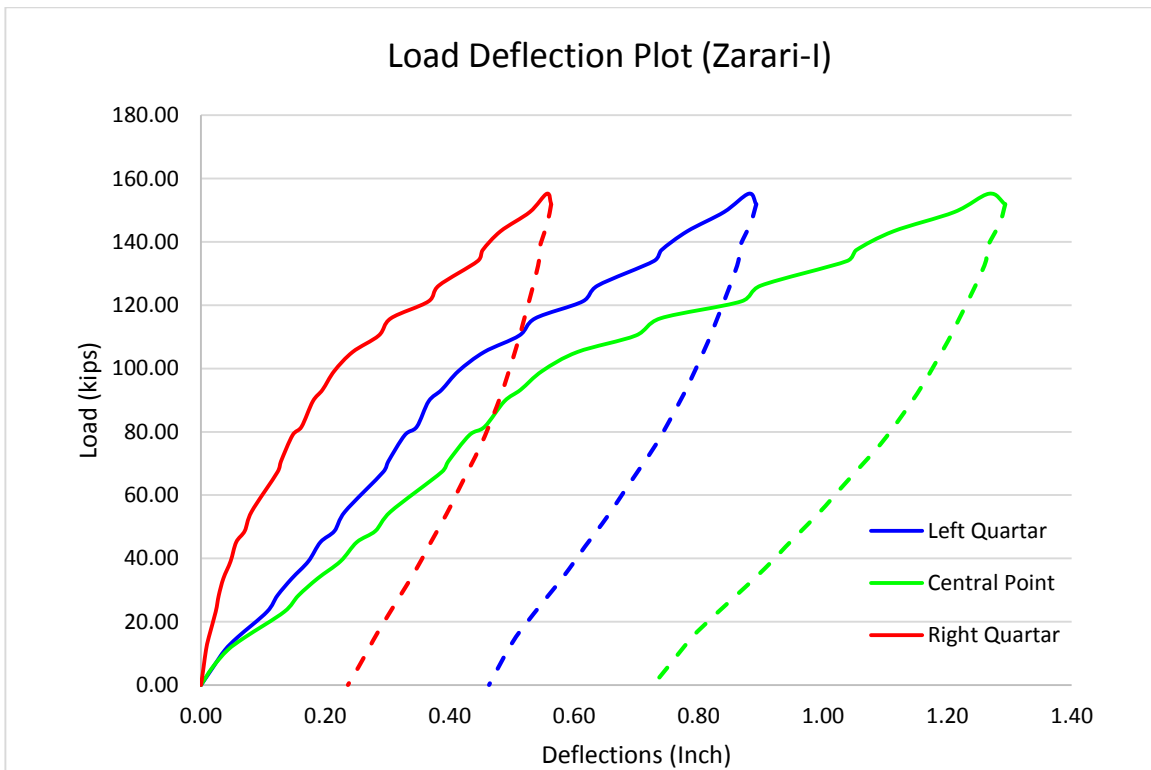
Figure 4-13: Load Deflection Plot of Z-I
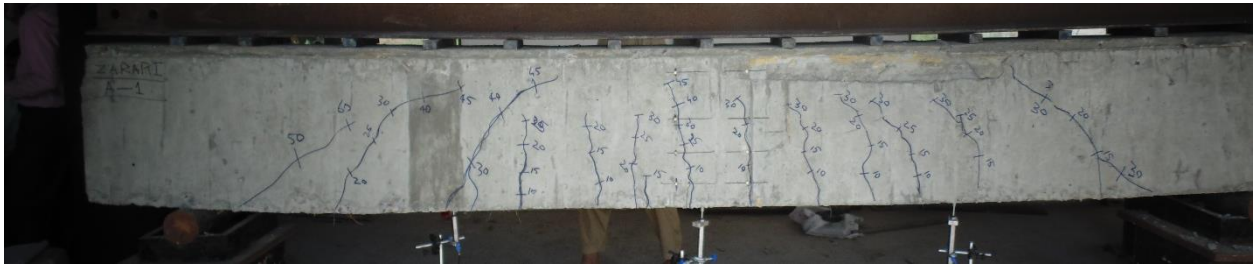
Figure 4-14: Cracked Pattern of Z-I

Table 4.6 Load Deflection Data of Beam Zarari's-I

Load Cell		Deflections					
		Left Quarter		Central Point		Right Quarter	
Tons	(Kips)	mm	Inch	mm	Inch	mm	Inch
0.00	0.00	0.00	0.00	0.00	0.00	0.00	0.00
2.70	5.94	0.17	0.01	0.67	0.03	0.15	0.01
5.47	12.07	0.48	0.02	1.36	0.05	0.29	0.01
7.87	17.35	0.97	0.04	2.09	0.08	0.42	0.02
10.17	22.41	1.54	0.06	2.95	0.12	0.59	0.02
15.40	33.94	3.27	0.13	5.30	0.21	1.24	0.05
17.84	39.31	3.68	0.14	5.86	0.23	1.45	0.06
20.06	44.22	4.69	0.18	7.16	0.28	2.01	0.08
22.70	50.04	5.13	0.20	7.71	0.30	2.28	0.09
25.06	55.23	5.64	0.22	8.38	0.33	2.64	0.10
27.02	59.55	6.28	0.25	9.12	0.36	3.05	0.12
30.62	67.49	7.57	0.30	10.84	0.43	4.16	0.16
32.30	71.19	7.82	0.31	11.17	0.44	4.36	0.17
35.20	77.58	8.74	0.34	12.35	0.49	5.16	0.20
37.61	82.89	9.37	0.37	13.22	0.52	5.73	0.23
40.38	89.01	9.83	0.39	13.83	0.54	6.11	0.24
42.73	94.17	10.55	0.42	14.79	0.58	6.75	0.27
45.01	99.20	11.07	0.44	15.49	0.61	7.18	0.28
45.01	99.20	11.07	0.44	15.49	0.61	7.18	0.28
47.48	104.64	11.82	0.47	16.50	0.65	7.82	0.31
50.13	110.48	12.74	0.50	17.89	0.70	8.59	0.34
52.16	114.97	13.69	0.54	19.38	0.76	9.42	0.37
55.09	121.41	15.04	0.59	21.65	0.85	10.59	0.42
57.15	125.97	16.13	0.63	23.49	0.92	11.60	0.46

|							
57.79	127.37	16.31	0.64	23.79	0.94	11.76	0.46
60.20	132.68	17.53	0.69	26.12	1.03	12.92	0.51
57.50	126.73	18.36	0.72	27.89	1.10	13.76	0.54
56.79	125.17	18.29	0.72	27.81	1.09	13.71	0.54
53.20	117.25	17.92	0.71	27.33	1.08	13.42	0.53
50.69	111.72	17.66	0.70	27.00	1.06	13.22	0.52
46.59	102.68	17.20	0.68	26.39	1.04	12.85	0.51
42.33	93.28	16.69	0.66	25.69	1.01	12.44	0.49
40.34	88.92	16.45	0.65	25.37	1.00	12.25	0.48
36.83	81.18	15.97	0.63	24.72	0.97	11.86	0.47
33.07	72.88	15.41	0.61	23.97	0.94	11.41	0.45
29.79	65.66	14.87	0.59	23.26	0.92	10.98	0.43
28.12	61.98	14.55	0.57	22.84	0.90	10.73	0.42
25.35	55.88	14.00	0.55	22.10	0.87	10.29	0.41
22.60	49.80	13.44	0.53	21.35	0.84	9.84	0.39
19.94	43.95	12.89	0.51	20.61	0.81	9.39	0.37
17.50	38.56	12.35	0.49	19.89	0.78	8.95	0.35
15.32	33.77	11.86	0.47	19.22	0.76	8.55	0.34
12.23	26.96	11.13	0.44	18.23	0.72	7.94	0.31
10.36	22.83	10.68	0.42	17.64	0.69	7.58	0.30
8.13	17.91	10.16	0.40	16.91	0.67	7.13	0.28
4.85	10.69	9.28	0.37	15.69	0.62	6.36	0.25
2.40	5.30	8.57	0.34	14.68	0.58	5.73	0.23
0.00	0.00	7.90	0.31	13.60	0.54	4.97	0.20
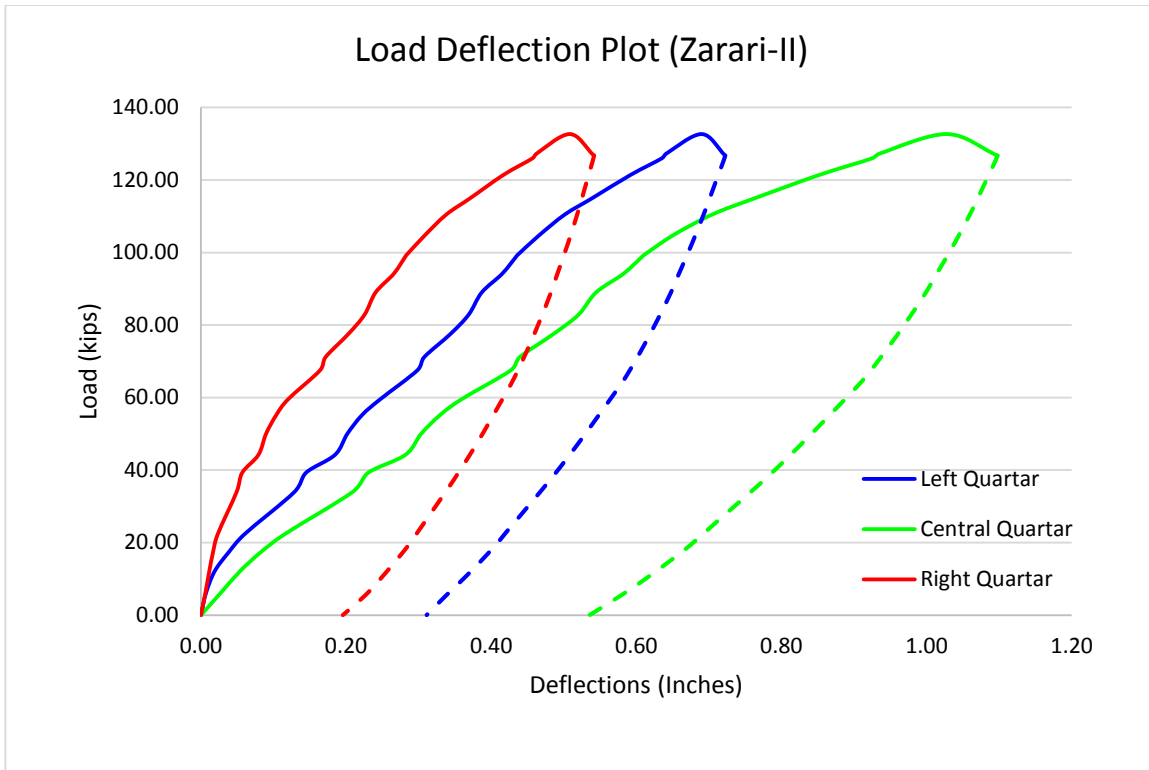
Figure 4-15: Load Deflection Plot of Z-II

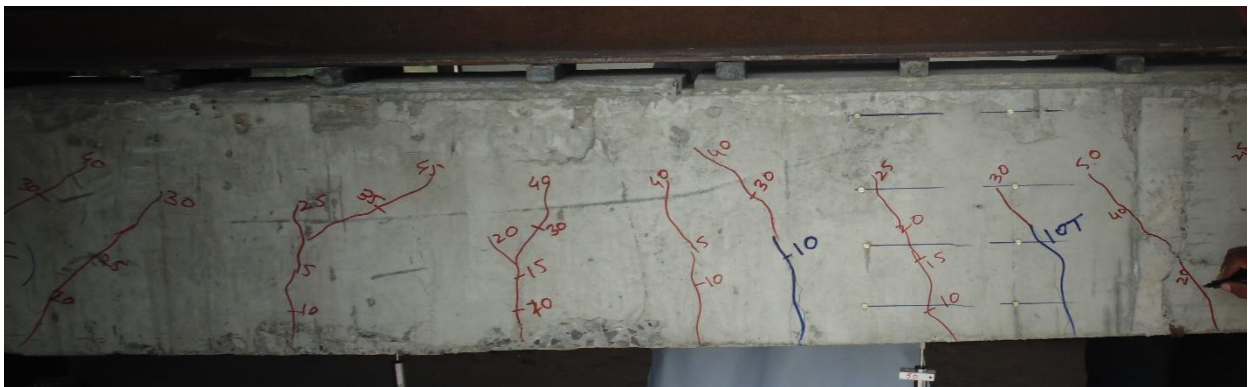Figure 4-16: Cracked Pattern of Z-II

Table 4.7 Load Deflection Data of Beam Modified Zarari's-I

Load Cell		Deflections					
		Left Quarter		Central Point		Right Quarter	
Tons	(Kips)	mm	Inch	mm	Inch	mm	Inch
0.00	0.00	0.00	0.00	0.00	0.00	0.00	0.00
2.51	5.53	0.12	0.00	0.37	0.01	0.41	0.02

5.57	12.29	0.42	0.02	0.82	0.03	0.80	0.03
7.44	16.40	0.98	0.04	1.35	0.05	1.11	0.04
10.61	23.39	1.82	0.07	2.32	0.09	1.69	0.07
12.98	28.60	3.00	0.12	3.54	0.14	2.42	0.10
14.84	32.70	3.49	0.14	4.16	0.16	2.81	0.11
17.55	38.68	4.26	0.17	5.10	0.20	3.40	0.13
20.02	44.12	5.23	0.21	6.31	0.25	4.25	0.17
22.86	50.38	5.94	0.23	7.20	0.28	4.83	0.19
25.09	55.30	6.61	0.26	8.02	0.32	5.37	0.21
27.63	60.90	8.46	0.33	9.62	0.38	6.35	0.25
30.80	67.88	9.51	0.37	10.87	0.43	7.15	0.28
32.97	72.67	10.00	0.39	11.46	0.45	7.54	0.30
35.02	77.19	11.23	0.44	12.65	0.50	8.29	0.33
37.60	82.87	12.08	0.48	13.55	0.53	8.88	0.35
40.30	88.83	13.28	0.52	14.77	0.58	9.65	0.38
42.28	93.19	13.89	0.55	15.46	0.61	10.10	0.40
45.32	99.89	14.71	0.58	16.42	0.65	10.72	0.42
53.40	117.70	17.77	0.70	20.63	0.81	13.44	0.53
55.49	122.30	18.27	0.72	21.34	0.84	13.91	0.55
57.56	126.87	20.52	0.81	24.77	0.98	16.04	0.63
60.21	132.70	21.64	0.85	26.36	1.04	17.00	0.67
62.54	137.84	23.02	0.91	28.19	1.11	18.04	0.71
65.03	143.32	25.34	1.00	30.94	1.22	19.60	0.77
63.45	139.85	25.72	1.01	31.24	1.23	19.75	0.78
59.79	131.78	25.28	1.00	30.85	1.21	19.46	0.77
57.71	127.19	25.07	0.99	30.58	1.20	19.29	0.76
54.90	121.00	24.77	0.98	30.20	1.19	19.06	0.75
51.06	112.54	24.35	0.96	29.65	1.17	18.72	0.74
49.48	109.05	24.15	0.95	29.40	1.16	18.57	0.73
47.91	105.60	23.97	0.94	29.16	1.15	18.42	0.73
45.02	99.23	23.61	0.93	28.68	1.13	18.12	0.71
42.03	92.64	23.21	0.91	28.16	1.11	17.80	0.70
40.09	88.35	22.93	0.90	27.79	1.09	17.58	0.69
37.11	81.79	22.50	0.89	27.21	1.07	17.22	0.68
35.93	79.20	22.29	0.88	26.93	1.06	17.05	0.67
32.42	71.45	21.70	0.85	26.13	1.03	16.56	0.65
30.40	67.00	21.30	0.84	25.59	1.01	16.23	0.64
26.46	58.33	20.49	0.81	24.51	0.97	15.56	0.61
24.35	53.67	20.04	0.79	23.93	0.94	15.19	0.60
22.57	49.75	19.65	0.77	23.41	0.92	14.86	0.59
20.64	45.48	19.21	0.76	22.83	0.90	14.49	0.57

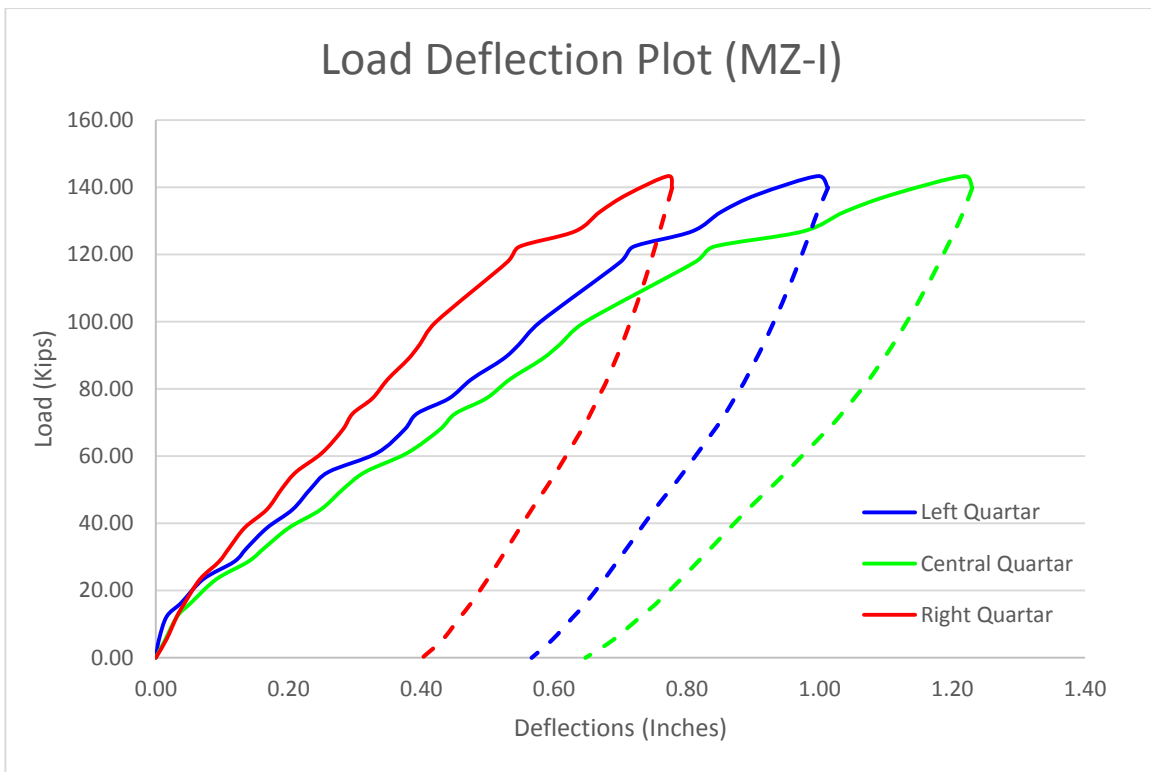| 17.38	38.31	18.54	0.73	21.93	0.86	13.90	0.55
15.58	34.34	18.18	0.72	21.46	0.84	13.58	0.53
12.03	26.51	17.45	0.69	20.49	0.81	12.95	0.51
10.35	22.81	17.10	0.67	20.02	0.79	12.64	0.50
7.21	15.90	16.41	0.65	19.12	0.75	12.03	0.47
5.33	11.74	15.92	0.63	18.48	0.73	11.60	0.46
2.42	5.33	15.16	0.60	17.51	0.69	10.96	0.43
0.00	0.00	14.38	0.57	16.45	0.65	10.19	0.40

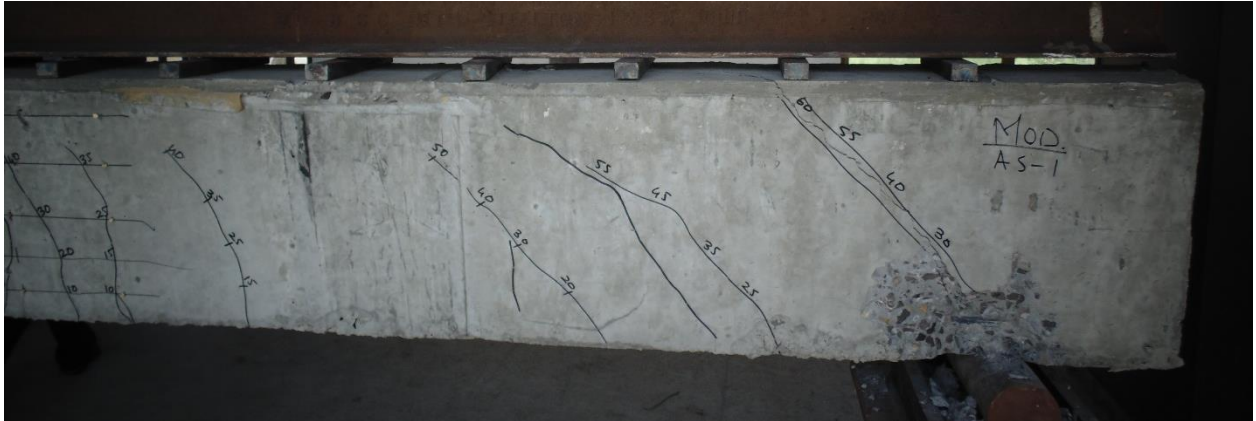*Figure 4-17: Load Deflection Plot of MZ-I*

Figure 4-18: Cracked Pattern of MZ-I

Figure 4-19: Cracked Pattern of MZ-I (Right Side)

Table 4.8 Load Deflection Data of Beam Modified Zarari's-II

Load Cell		Deflections					
		Left Quarter		Central Point		Right Quarter	
Tons	(Kips)	mm	Inch	mm	Inch	mm	Inch
0.00	0.00	0.00	0.00	0.00	0.00	0.00	0.00
2.69	5.94	0.31	0.01	0.49	0.02	0.21	0.01
5.35	11.79	0.71	0.03	0.97	0.04	0.41	0.02
7.68	16.92	1.19	0.05	1.59	0.06	0.66	0.03
10.94	24.10	2.03	0.08	2.77	0.11	1.17	0.05
12.06	26.58	2.25	0.09	3.06	0.12	1.31	0.05
14.86	32.76	2.89	0.11	3.89	0.15	1.71	0.07
17.48	38.53	3.47	0.14	4.67	0.18	2.15	0.08
20.67	45.56	4.27	0.17	5.68	0.22	2.70	0.11
22.16	48.83	4.80	0.19	6.35	0.25	3.12	0.12
25.35	55.87	5.68	0.22	7.44	0.29	3.75	0.15
27.39	60.37	6.00	0.24	7.84	0.31	3.98	0.16
29.97	66.05	6.52	0.26	8.50	0.33	4.37	0.17
32.18	70.93	7.42	0.29	9.49	0.37	4.96	0.20
35.96	79.25	8.18	0.32	10.43	0.41	5.52	0.22
37.02	81.60	8.53	0.34	10.86	0.43	5.79	0.23
40.37	88.97	9.38	0.37	11.85	0.47	6.40	0.25
42.81	94.36	10.04	0.40	12.80	0.50	7.02	0.28
45.00	99.17	10.61	0.42	13.49	0.53	7.45	0.29
47.62	104.96	11.22	0.44	14.22	0.56	7.90	0.31
50.51	111.32	11.83	0.47	15.04	0.59	8.39	0.33
52.41	115.51	12.94	0.51	16.79	0.66	9.24	0.36

|							
55.38	122.05	13.78	0.54	18.03	0.71	9.86	0.39
57.25	126.19	14.69	0.58	19.48	0.77	10.51	0.41
60.65	133.68	16.10	0.63	21.66	0.85	11.58	0.46
62.15	136.97	17.05	0.67	23.08	0.91	12.26	0.48
64.15	141.40	17.76	0.70	24.15	0.95	12.78	0.50
62.84	138.50	18.42	0.73	25.05	0.99	13.18	0.52
60.24	132.78	18.18	0.72	24.78	0.98	13.01	0.51
54.41	119.92	17.61	0.69	24.09	0.95	12.60	0.50
52.46	115.62	17.40	0.68	23.84	0.94	12.45	0.49
52.46	115.62	17.40	0.68	23.84	0.94	12.45	0.49
46.25	101.94	16.67	0.66	22.93	0.90	11.92	0.47
43.29	95.41	16.25	0.64	22.40	0.88	11.61	0.46
39.53	87.13	15.66	0.62	21.66	0.85	11.18	0.44
37.97	83.69	15.39	0.61	21.31	0.84	10.98	0.43
34.53	76.10	14.77	0.58	20.51	0.81	10.52	0.41
30.91	68.12	14.07	0.55	19.59	0.77	10.00	0.39
27.21	59.96	13.35	0.53	18.62	0.73	9.45	0.37
25.02	55.14	12.91	0.51	18.03	0.71	9.12	0.36
21.59	47.58	12.21	0.48	17.09	0.67	8.58	0.34
17.99	39.64	11.44	0.45	16.06	0.63	7.99	0.31
15.00	33.06	10.78	0.42	15.22	0.60	7.49	0.29
12.55	27.67	10.26	0.40	14.54	0.57	7.09	0.28
10.71	23.60	9.81	0.39	13.97	0.55	6.75	0.27
7.34	16.18	9.04	0.36	13.00	0.51	6.18	0.24
5.86	12.91	8.69	0.34	12.57	0.49	5.92	0.23
2.57	5.66	7.91	0.31	11.59	0.46	5.32	0.21
0.00	0.00	7.14	0.28	10.64	0.42	4.72	0.19
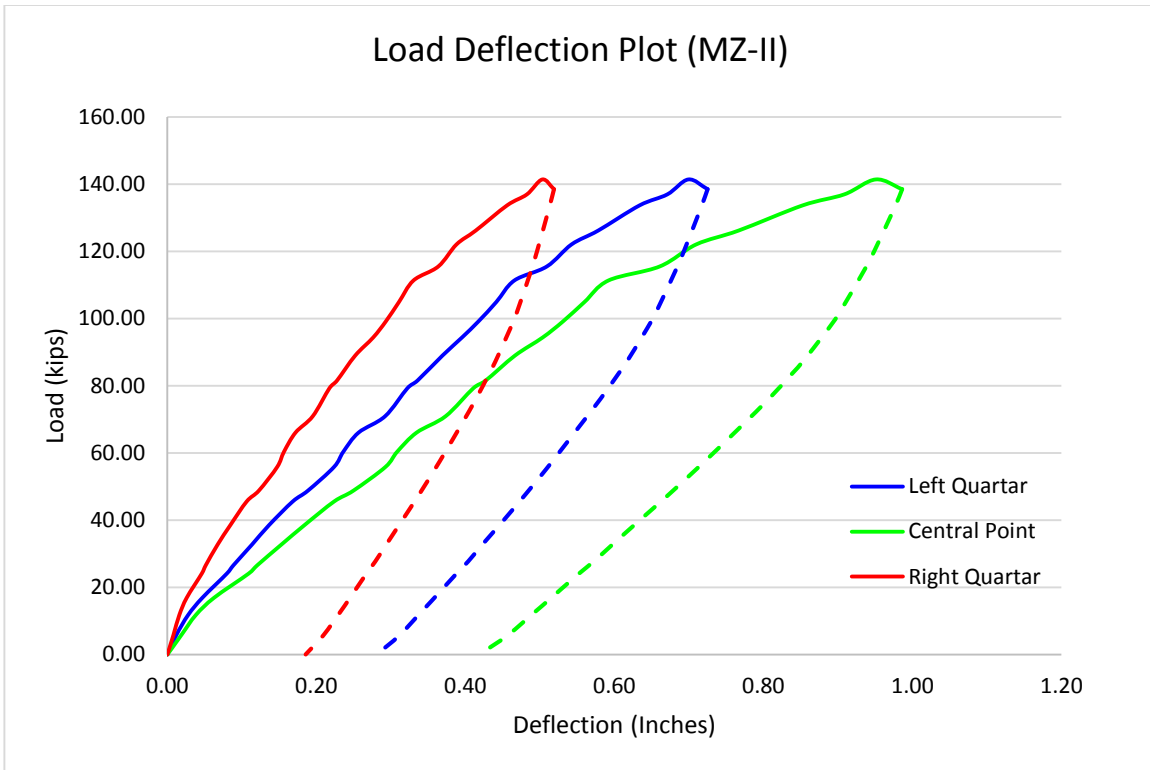
Figure 4-20: Load Deflection Plot of MZ-II

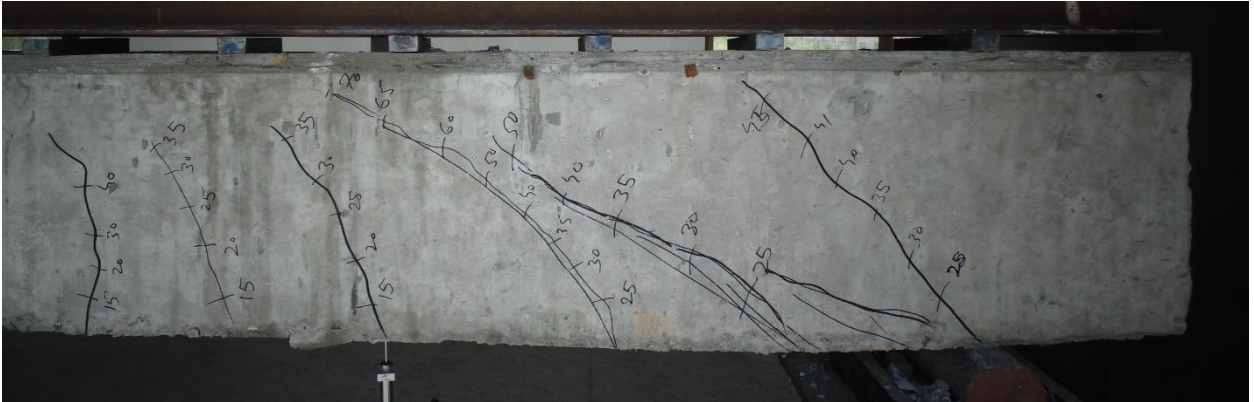*Figure 4-21: Cracked Pattern of MZ-II*

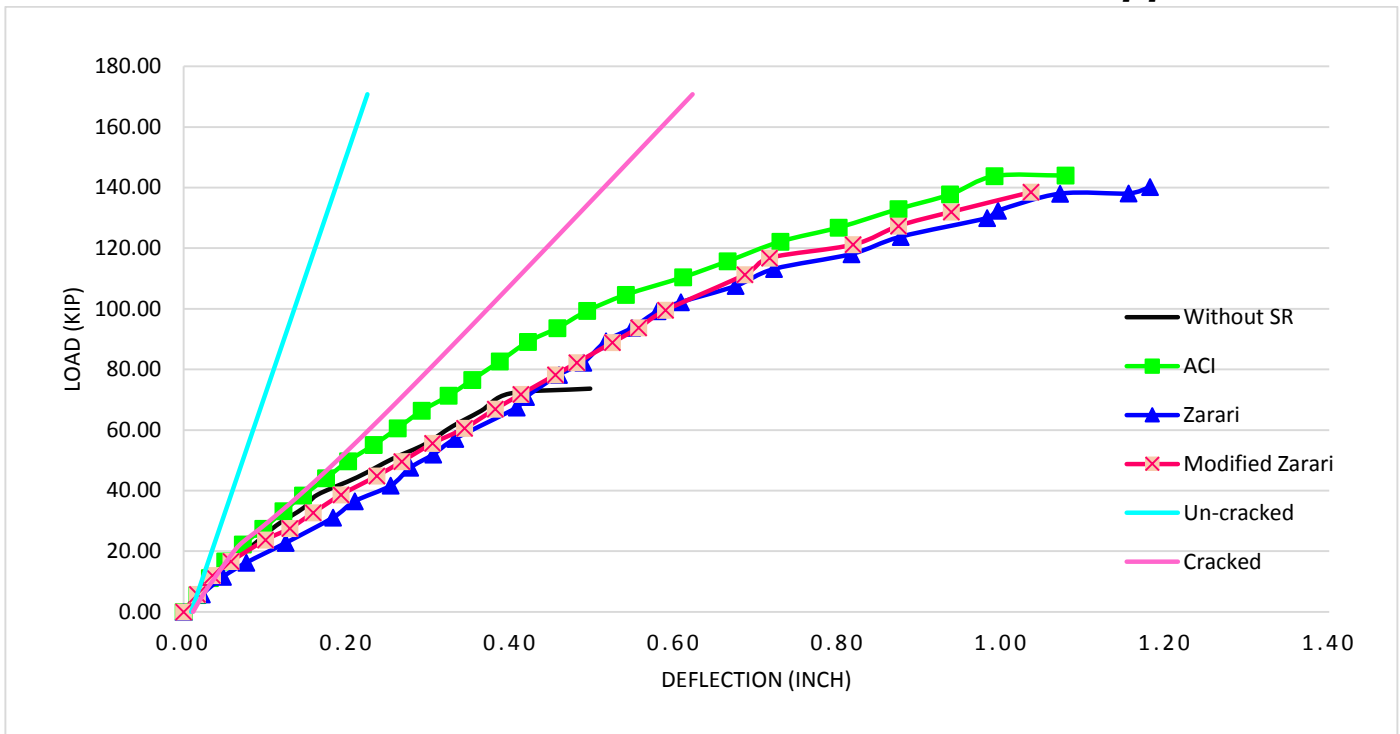*Figure 4-22: Cracked Pattern of MZ-II (Right Side)*

Figure 5-1 : Load Deflection Response of Beams

Beam	Experimental Strength (Kips)			ACI Predicted Strength (Kips)			Value of γ
	Vc	Vs	Vu	Vc	Vs	Vu	
N1	36.64	0	36.64	20.61	0	20.61	3.55
N2	39.20	0	39.20	20.61	0	20.61	3.80
						Mean	3.68
A1	67.19	8.36	75.55	20.61	8.36	28.98	6.52
A2	63.82	8.36	72.18	20.61	8.36	28.98	6.19
						Mean	6.36
Z1	55.95	21.66	77.62	20.61	21.66	42.28	5.43
Z2	44.68	21.66	66.34	20.61	21.66	42.28	4.33
						Mean	4.88
M1	57.72	13.94	71.66	20.61	13.94	34.55	5.60
M2	56.76	13.94	70.70	20.61	13.94	34.55	5.51
							5.55

Table 5-1: Experimental Values of "γ" for concrete shear strength
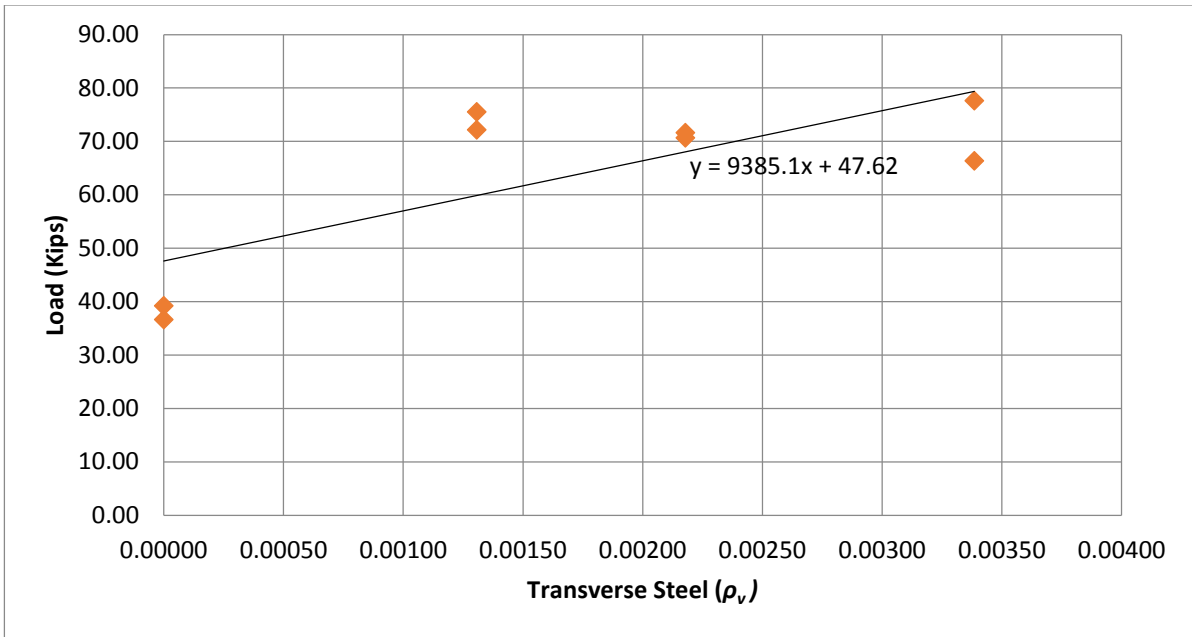
Figure 5-2: Transverse Steel Ratio Vs Ultimate Shear Strengths Comparison of Specimens
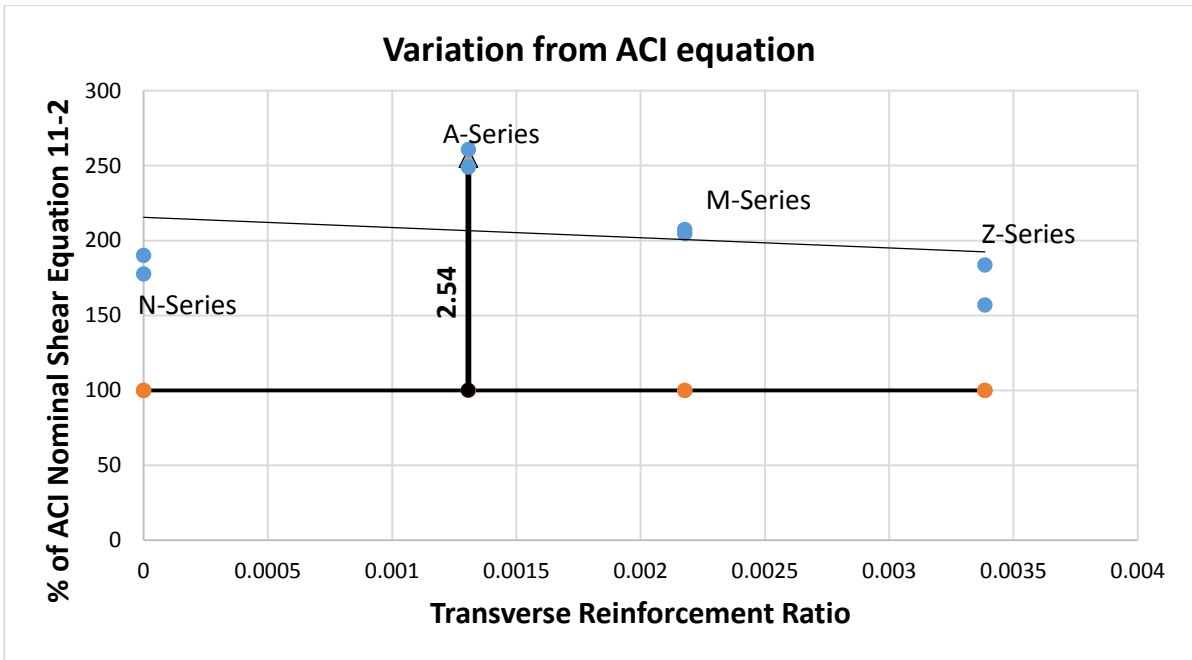

Figure 5-3: Variation in Experimental Shear Strength from ACI Theoretically calculated Shear Strengths
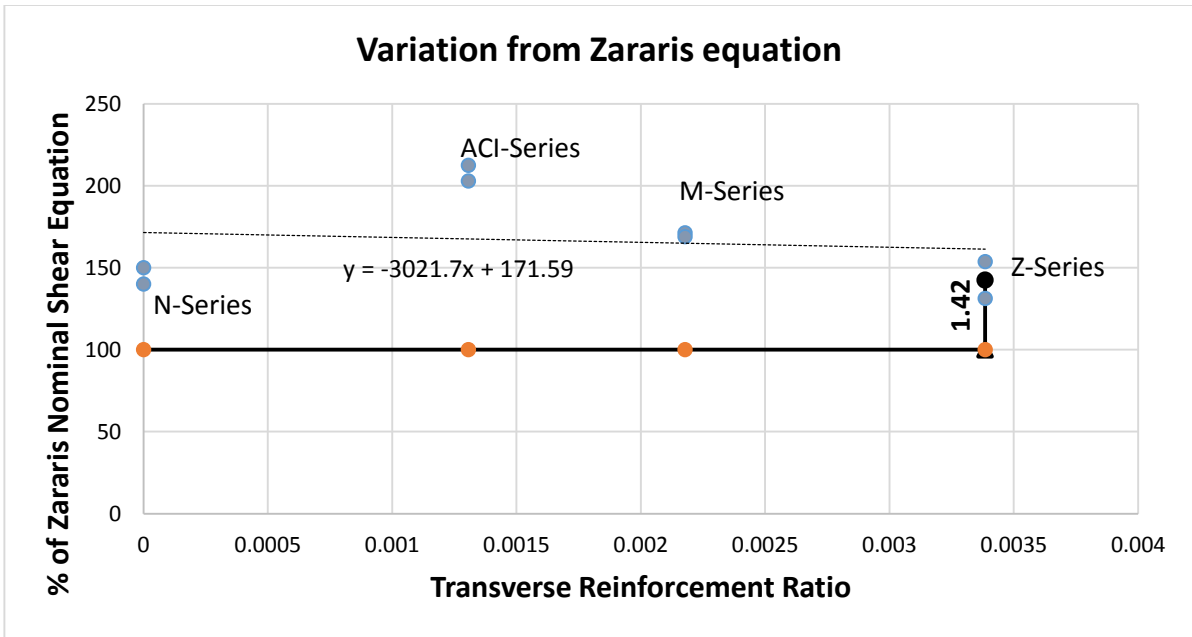
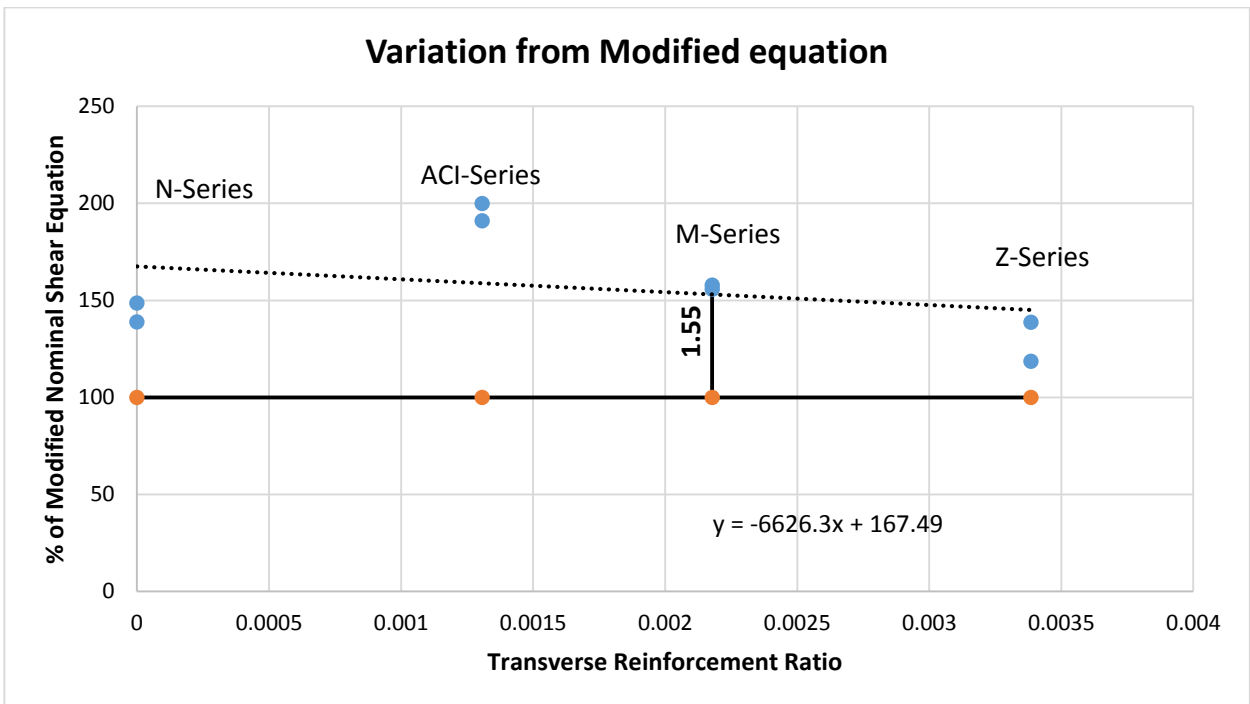*Figure 5-4: Variation in Experimental Shear Strength from Zarari's Eq.*

Figure 5-5: Variation in Experimental Shear Strength from Modified Zarari's Eq.
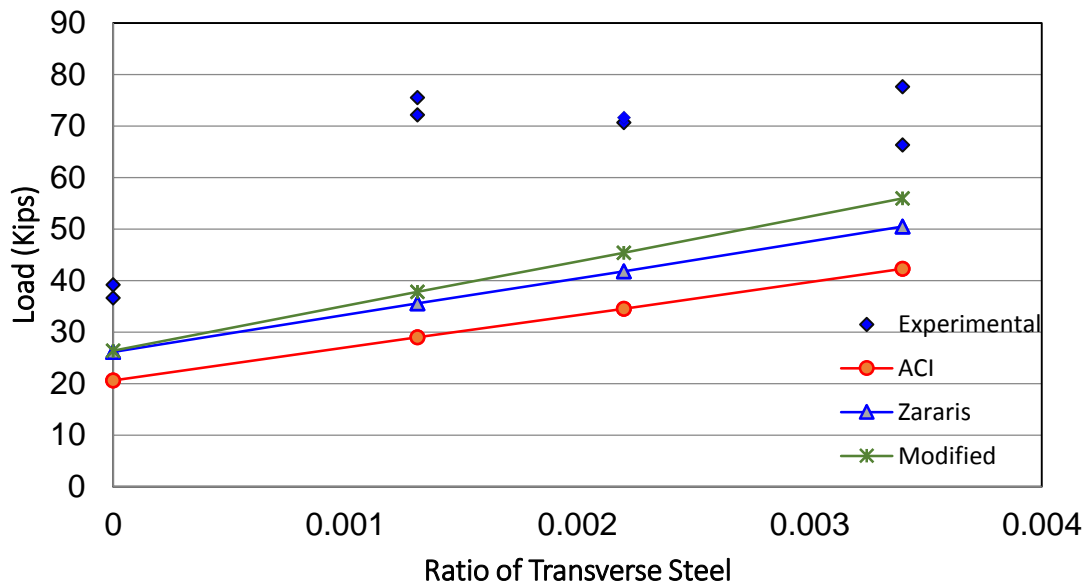
Figure 5-6: Transverse Steel Ratio Vs Ultimate Shear Strengths Comparison of Specimens

Experimental Vexp (Kips)	ACI 318-11		Zararis Equation		Modified Equation	
	Vaci (Kips)	Vexp/Vaci	Vzar (Kips)	Vexp/Vzar	Vmod (Kips)	Vexp/Vmod
36.64	20.61	1.778	26.14	1.402	26.382	1.389
39.20	20.61	1.902	26.14	1.500	26.382	1.486
37.92	20.610	1.840	26.139	1.451	26.382	1.437
75.55	28.97	2.608	35.55	2.125	37.806	1.998
72.18	28.97	2.492	35.55	2.031	37.806	1.909
73.87	28.970	2.550	35.546	2.078	37.806	1.954
77.62	42.27	1.836	50.51	1.537	55.97	1.387
66.34	42.27	1.569	50.51	1.314	55.97	1.185
71.98	42.270	1.703	50.507	1.425	55.972	1.286
71.66	31.54	2.272	41.82	1.714	45.42	1.578
70.70	34.54	2.047	41.82	1.691	45.42	1.556
71.18	33.040	2.159	41.818	1.702	45.422	1.567
		2.06		1.66		1.55

Table 5-2: Shear Strengths of Specimens
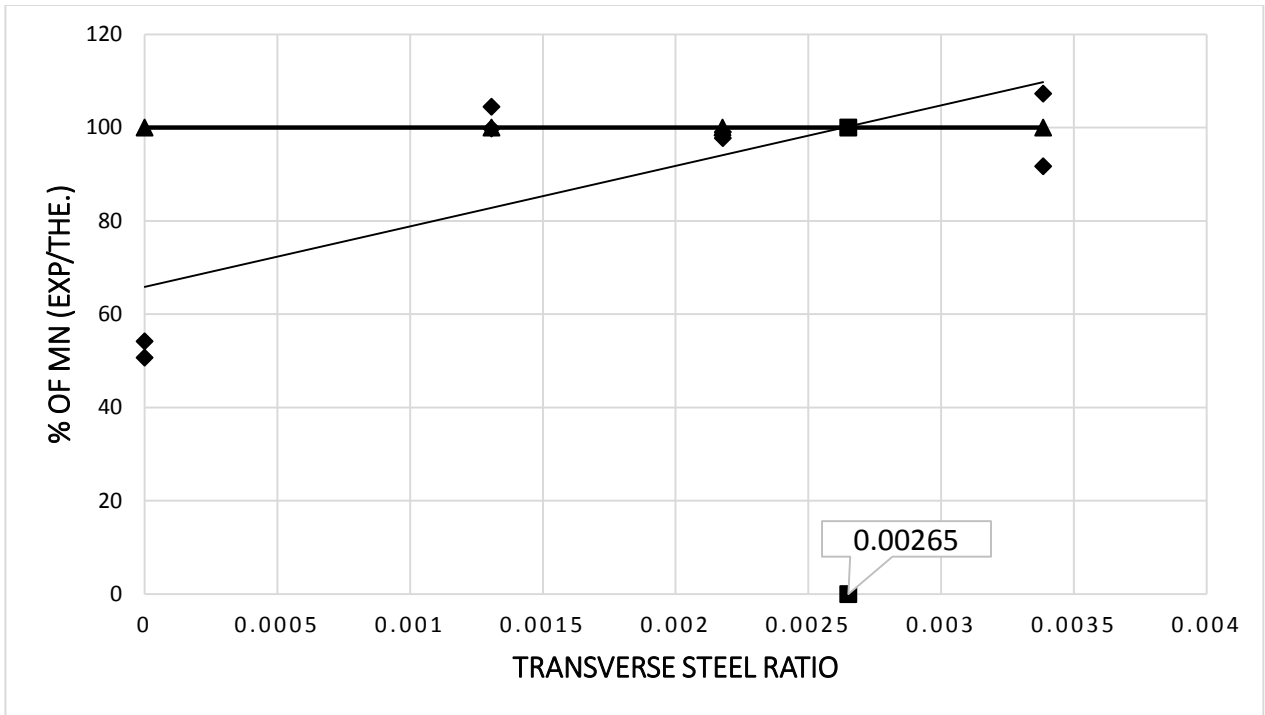
Figure 5-7: Transverse Steel Ration vs Achieved Moment Capacity.

1	2 (Kashif)			3 (Talha)			4 (Babar)		
Max Shear in UDL Case (kip)	Max Shear (Shear Span= 40")	Moment (k-in)	"a" for UDL (Inch)	Max Shear (Shear Span= 48")	M (k-in)	"a" for UDL (Inch)	Max Shear (Shear Span = 52")	M (k-in)	"a" for UDL (Inch)
36.64	27.60	1104.00	30.13	19.14	918.79	25.08	19.14	995.28	27.16
39.20	27.60	1104.00	28.16	20.00	960.18	24.49	20.00	1040.00	26.53
75.55	45.70	1828.00	24.20	43.07	2067.54	27.37	34.71	1804.92	23.89
72.18	46.90	1876.00	25.99	43.61	2093.48	29.00	35.25	1833.00	25.39
77.62	65.10	2604.00	33.55	47.24	2267.45	29.21	29.64	1541.28	19.86
66.34	64.80	2592.00	39.07	44.34	2128.54	32.09	26.74	1390.48	20.96
71.66	54.70	2188.00	30.53	44.09	2116.15	29.53	32.68	1699.36	23.71
70.70	53.30	2132.00	30.16	47.45	2277.37	32.21	36.04	1874.08	26.51
		a=	30.22		a=	28.62		a=	24.25
		a/d	1.89		a/d	1.79		a/d	1.52

Table 5-3: Shear Span for UDL Loading

REFERENCES

[1]   Mörsch, E., "Concrete-Steel Construction", McGraw-Hill, New York (English

translation by E.P. Goodrich).

[2]   Ritter, W., "Die bauweise bennebique", Schweizerische Bauzeitung, Vol 33, No
7,1899, pp. 59-61.

[3]   Jame. K. Weight and James G Macgregor (2005). Reinforced concrete members

[4]   Kani, G. (1964). The Riddle of Shear Failure and Its Solutions. ACI Journal , 61
(4), 441-467.

[5]   Prodromos D. Zarais, "Shear Strength and Minimum Shear Reinforcement of
Reinforced Concrete Slender Beams," ACI Structural Journal, V. 100, No. 2,
March – April 2003, pp. 203 – 214.

[6]   Collins, M., Bentz, E., Sherwood, E., & Xie, L. (2007). An adequate theory for the
shear strength of reinforced concrete structures.

[7]   Braestrup, M. (2009). Structural Concrete Beam Shear - Still a Riddle? ACI
Special Publication , 265, 327-344.

[8]   Collins, M. P., and Mitchell, D., "A Rational Approach to Shear Design-The 1984
Canadian Code Provisions." ACI Journal, Vol 83, No 6, 1986, pp. 925-933.

[9]   Adebar, P., "Testing Structural Concrete Beam Elements", RILEM: Mat. And

Struct., Vol 27, No 172, 1994, pp. 445-451.

[10]   Leonhardt, F., & Walther, R. (1961-1962). Contribution to the treatment of shear
in reinforced concrete (Vol. Technical Translation 1172). (J. Verschuren, & J.
MacGregor, Trans.) National Research Council of Canada.

[11]   Kani, G. (1967). How safe are our large reinforced concrete beams. ACI Journal
64 (3), 128-141.

[12]   Gupta, P., Collins, M.P., "Behavior of Reinforced Concrete Members Subjected to Shear and Compression", Report, Department of Civil Engineering, University of Toronto,Canada, 1993.

[13]   Mattock, A.H., "Diagonal Tension Cracking in Concrete Beams with Axial Forces",

[14]   Jung-Yoon Lee and Uk-Yeon Kim, "Effect of Longitudinal Tensile Reinforcement Ratio and Shear Span-Depth Ratio on Minimum Shear Reinforcement in Beams," ACI Structural Journal, V. 105, No. 2, March – April 2008, pp. 134 – 144.

[15]   Taylor, H.P.J., "Investigation of the Forces Carried Across Cracks in Reinforced Concrete Beams in Shear by Interlock of Aggregate", Cement and Concrete Association, London, 1970, 22 pp.

[16]   König, G, Grimm, R., Remmel, G., "Shear Behavior of Longitudinally Reinforced Concrete Members of HSC", Darmstadt Concrete, Vol. 8, 1993, pp. 27-42.

[17]   Pendyala, R.S., Mendis, P., "Experimental Study on Shear Strength of High-Strength Concrete Beams", ACI Structural Journal, Vol. 97, No4, 2000, pp. 564.

[18]   Reineck, K.-H., Kuchma, D., Kim, K.S., and Marx, S., "Shear Database for Reinforced Concrete Members without Shear Reinforcement", ACI Structural Journal, Vol 100, No 2, 2003, pp. 240-249.

[19]   Ziara, M. M. (1993). The influence of confining the compression zone in the design of structural concrete beams. Heriot-Watt University.

[20]   Jansen and A. Lapko, "On Shear Reinforcement Design of Structural Concrete Beams on the Basis of Theory of Plasticity," Journal of Civil Engineering and Management, V. 15, No. 4, 2009, pp. 395 – 403.

[21]   Alexander Placas and Paul E. Regan, "Shear Failure of Reinforced Concrete Beams," ACI Journal, 1971, pp. 763 – 773.

[22]   Evan C. Bentz, Frank J. Vecchio and Michael P. Collins, "Simplified Modified Compression Field Theory for Calculating Shear Strength of Reinforced Concrete Elements," ACI Structural Journal, V. 103, No. 4, July –August 2006, pp. 614 – 624.

[23]   Aurelio Muttoni and Miguel F. Ruiz, "Shear Strength of Members without Transverse Reinforcement as Function of Critical Shear Crack Width," ACI Structural Journal, V. 105, No. 2, March – April 2008, pp. 163 – 172.